102

CHAOTIC BEHAVIOR OF DETERMINISTIC SYSTEMS

A THESIS SUBMITTED IN PARTIAL FULFILLMENT FOR THE REQUIREMENTS OF THE DEGREE MASTER OF SCIENCE IN PHYSICS IN ADDIS ABABA UNIVERSITY

By

Tsegaye Takele

June, 1989

Addis Ababa

ACKNOWLEDGEMENT

I offer my deepest gratitude to my advisor Dr. J. Jelen for his consistent supervision, limitless effort and dedication in guiding the work. His deep knowledge and rich experience in the field facilitated my progress in the thesis work.

I am also very grateful to W/O Azeb Belay for her help in preparing the technical part of the thesis.

Finally, I gratefully acknowledge all those who gave me assistance in the realization of this work.

CONTENTS

	Page
INTRODUCTION	1
1. Experiments and Simple Models	3
1.1 Experiments Leading to Deterministic Chaos	3
1.1.1 Periodically driven Pendulum	3
1.1.2 Benard Experiment	4
1.1.3 Belousov-Zhabotinsky Reaction	6
1.1.4 Henon-Heiles System	7
1.2 One-dimensional Noninvertible Maps	8
1.3 Characterization of Chaotic Motion	12
1.3.1 Liapunov Exponent	12
1.3.2 The Invariant Measure	13
1.3.3 Correlation Function	15
2. Universal Properties of Quadratic Maps	17
2.1 The Logistic Map	18
2.1.1 Mechanism of Peirod Doubling (Pitchfork Bifurcation)	20
2.1.2 Chaotic Region	27
2.1.3 Power Spectrum	28
2.2 Experimental support for Feignbaum Route	29
2.2.1 Onset of Turbulence	29
2.2.2 Nonlinear RCL-Oscillator	32
3. The Intermittency Route to Chaos	34
3.1 Mechanisms for Intermittency	34
3.1.1 Type-I Intermittency	35
3.2 Summary of the Measurable Properties of Intermittency Route	38
3.3 Experimental Evidence for Type-I Intermittency Route	39
3.3.1 Benard Experiment	40
3.3.2 Nonlinear RCL-Oscillator	40
3.3.3 Belousov-Zhabotinsky Reaction	41

Table of Content Contd.

	Page
4. Strange Attractors in Dissipative Dynamical Systems	
4.1 Introduction and Definition of a Strange Attractor	43
4.1.1 Dissipative Flows	43
4.1.2 Dissipative Maps	46
4.2 Strange Attractors and the onset of Turbulence	50
4.2.1 Landau's Route to Chaos	51
4.2.2 Ruelle-Takens-Newhouse Route to Chaos	52
4.3 Experimental Evidence for Ruelle-Takens-Newhouse Route to Chaos	53
4.3.1 Benard Experiment	54
4.3.2 Benard Instability	54
4.3.3 Taylor Instability	55
4.4 Summary of Routes to Chaos	56
5. Chaos in Conservative Systems	58
5.1 Non-Integrable Versus Integrable Hamiltonian Mechanics	58
5.2 Properties of Integrable Systems	61
5.3 Sensitive Dependence on Initial Conditions and Random Behavior	63
5.4 Examples of Classical Chaos	65
6. Chaos in Nature Outside Physics	68
7. Conclusion and Implicaitons	69
Reference	71

ABSTRACT

We have considered nonlinear systems whose time dependence is deterministic and presented some representative physical systems which display chaotic behavior. Simple model maps which can exhibit chaos similar to the chaos observed in more complex systems are studied. Characterization for one dimensional maps whether they are chaotic or not are given quantitatively. The three known prominent scenarios, and their accompaning experiments, leading to chaos are analysed in some detail. Strange attractors in dissipative systems and their relevance to turbulence is considered. The appearance of chaos in conservative systems are shortly dealt. Finally, chaos in different branches of science and its implications are stated.

Chaotic Behavior of Deterministic Systems

Introduction

We often say 'given the initial conditions we know what a deterministic system will do far into the future'. Some people knew this was false in the past (Poincare 1892), and we know it is false in the following sense: given infinitesimally different starting points, we often end up with widely different outcomes. Almost all non-linear systems will exhibit such irregular or chaotic behavior.

We will consider systems whose time dependence is deterministic. That is, there exists a format in the form of differential or difference equations to calculate the behavior of the system from a given initial conditions. Therefore, chaotic behavior in deterministic system refers to chaotic motion which is generated by non linear systems whose dynamical law uniquely determine the time evolution of the state of the system from a knowledge of its previous history.

The observed chaotic behavior of these systems in time is neither due to external source of noise or to an infinite degrees of freedom nor to the uncertainity associated with quantum mechanics. The actual source of chaotic behavior is the property of the nonlinear system of separating initially close trajectories exponentially fast in a bounded region of phase space.

Therefore, it becomes impossible to predict the long time behavior of these systems, because in practice one can only fix their initial conditions with finite accuracy, and errors increase exponentially fast. In order to

predict for longer and longer times one has to put more and more digits on the initial conditions of these systems. Lorenz called this sensitive dependence on initial conditions the 'butterfly effect'.

These results will confront us with questions such as: can one predict whether or *not* a given system will display a deterministic chaos? What is this impact on different branches of Physics? etc. There are some answers to such type of questions. However, there are still more unsolved than solved problems in this field of deterministic chaos. Nevertheless, we will try to assess few questions pertaining to these deterministic systems.

We begin by presenting typical experiments and models which di-splay deterministic chaos. Then we will try to give mathematical characterization of chaotic motion for one dimensional maps. We will consider different routes leading to chaotic motion in dissipative systems. Latter we will consider chaos in conservative systems.

The most recent route to chaos is the Feignbaum route, which is developed from a consideration of simple difference equation. A second approach to chaos is the intermittency route which has been discovered by Manneville and Pomeau (1979). A third possibility was founded by Ruelle Takens and Newhouse (1978) All these three routes to chaos are supported by experiments.

Chaos in conservative systems is considered without mathematical proof. Finally, the existance of chaos in different fields and its implications are stated.

1. Experiments and Simple Models

In this section we will present some experiments and models which exhibit deterministic chaos. Based on this experiments we will try to characterize chaos qualitatively.

1.1 Experiments leading to deterministic chaos

1.1.1 Periodically driven pendulum

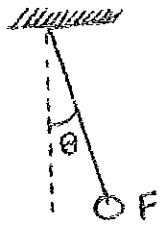

Fig. 1.1: Periodically driven pendulum

The equation of motion for periodically driven pendulum is

$$\ddot{\theta} + \gamma\dot{\theta} + g \sin\theta = F \cos wt \qquad (1.1)$$

where γ is the dampling constant, g is acceleration due to gravity w is frequency of the driving force. If we make a change of variables, $x = \theta$, $y = \dot{\theta}$ $z = wt$, we will obtain

$$\dot{x} = y$$

$$\dot{y} = -\gamma y - g \sin x + f \cos z$$

$$\dot{z} = w \qquad (1.2)$$

The mass is normalized to unity. This equation is numerically integrated for different sets of paramters (γ, g, w, F). It has been found that this simple system appears to be chaotic when F, the amplitude of the driving force exceeds a treshold value F_c [6].

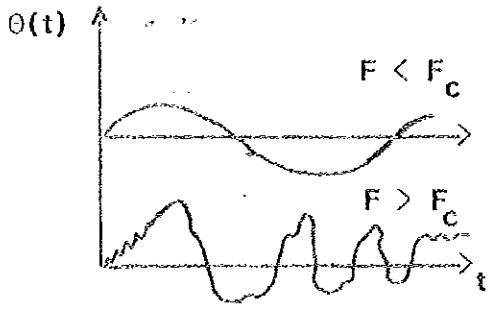

Fig. 1.2: θ versus t for regular and irregular motion

1.1.2 Benard Experiment

In the Benard experiment, a fluid layer is heated from below in a gravitational field.

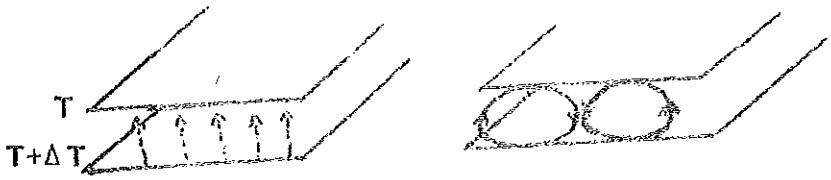

Fig. 1.3: Benard Experiment

The heated fluid at the bottom "wants" to rise, and the cold at the top "wants" to fall, but this motions are opposed by viscous forces. For small temperature difference ΔT, viscosity wins, the liquid remains at rest and heat is transported by uniform heat conduction. This state becomes unstable at a critical value R_a of the Rayleigh number R, which is proportional to ΔT, and a state of stationary convection rolls develops. If R increases a transition to chaotic motion is observed after a second threshold R_c. To measure experimentally the chaotic phenomena seen in the experiment, we make use of the power or frequency spectrum [1] of the velocity in the x-direction.

$p(\omega) = |f(\omega)|^2$, where $f(\omega)$ is the Fourier transform of $f(t)$.

From this expression of $p(\omega)$ it has been found that for periodic motion $p(\omega)$ consists of discrete lines, whereas chaotic motion is indicated by a broad continuum in $p(\omega)$ at low frequencies. This is clearly seen in Benard Experiment.

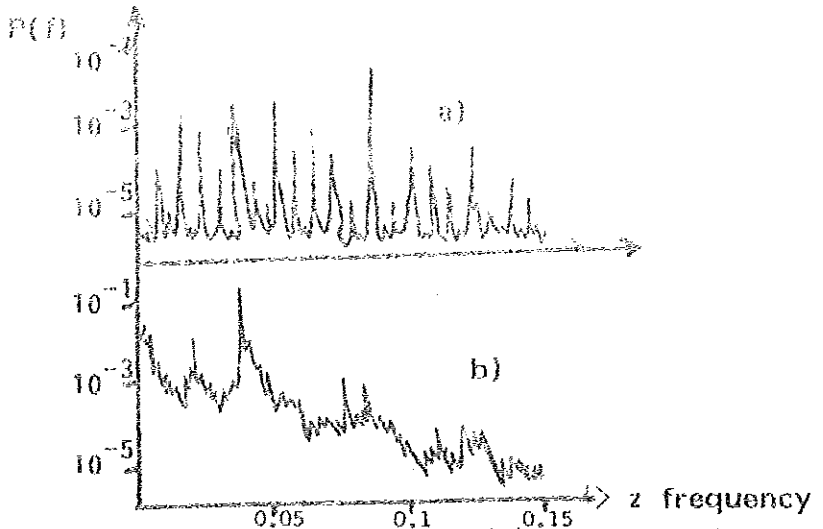

Fig. 1.4: Power spectrum for regular (a) and irregular motion (b).

To describe the Benard Experiment theoretically, Lorenz truncated the complicated differential equation which describe this system and obtained the following equation [2]:

$$\dot{X} = -\sigma X + \sigma Y$$

$$\dot{Y} = rX - Y - XZ$$

$$\dot{Z} = XY - bZ$$

where σ and b are dimensionless constants which characterize the system, and r is the control parameter which is proportional to ΔT. X is proportional to the circulatory fluid flow velocity, Y characterizes the temperature difference between ascending and descending fluid elements, and Z is proportional to the deviation of the vertical temperature profile from its equilibrium value.

A numberical analysis of the above equations, the Lorenz model, shows that its variables can exhibit chaotic motion above a threshold value r_c. It should be noted that the Lorenz equations describe the Benard experiment only in the immeidate vicinity of the transition from heat conduction to convection rolls, for the spatial Fourier Coefficients retained by Lorenz only describe simple rolls.

1.1.3 Belousov-Zhabotinsky Reaction

This is an example from chemistry. Previously if an experimentalist obtained a chaotic record in the study of chemical reactions, he would throw away the record, saying that the experiment was unsuccessful. Things, fortunately, have changed and we now have several examples of non periodic chemical reactions among them is Belousov-Zhabotinsky reaction.

The general equations for the concentrations $[C_i]$ of the reactants in a system of chemical reactions are again a set of first-order, non-linear differential equations:

$$\frac{d}{dt}\,\vec{x} = \vec{F}(\vec{x}, r)$$

where $\vec{x} = (C_1, C_2, \ldots, C_d)$, $\vec{F}$ is a nonlinear function of the $[C_i]$ and r denotes an external control parameter. The variable in the Belousov-Zhabotinsky reaction is the concentration C of the $C\,e^{4+}$-ions, which is measured via the selective light absorption of these ions. The mean residence time of the substance in the open reactor acts as an external control parameter.

The transition to chaos in this system is detected by the autocorrolation function.

$$\hat{C}(\tau) = \lim_{T\to\infty} \int_0^T dt\ \hat{C}(t)\ \hat{C}(t+\tau);\quad \hat{C}(t) = C(t) - \lim_{T\to\infty} \frac{1}{T} \int_0^T dt\ C(t) \qquad (1.4)$$

This function measures the correlation between subsequent signals. It remains constant or oscillates for regular motion and decays rapidly if the signal is chaotic.

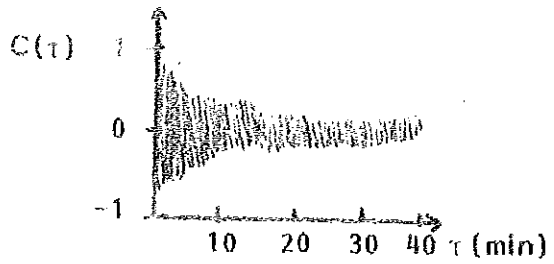

Fig. 1.5: Auto Correlation Function

One can use also frequency spectrum to distinguish whether the above reaction is choatic or not [3].

1.1.4 Henon-Heiles System

This is an example from classical mechanics which can exhibit chaos or regular motion depending on the energy of the system which acts as an external control parameter. Its Hamiltonian is given by

$$H = \tfrac{1}{2}(p_1^2 + q_1^2 + p_2^2 + q_2^2) + (q_1^2 q_2 - \frac{q_2^3}{3}) \qquad (1.5)$$

which consists of an integrable pair of harmonic oscillators coupled by non-integrable cubic terms. Its equationsof motion were first studied numerically by Henon and Heiles (1969). They used the Poincare map to distinguish between chaotic and regular motion. They found that for high enough energies the Poincare map for the Henon-Heiles system become plan-filling which implies the motion is chaotic. They plotted the points in which the trajectory in phase space $\vec{x}(t) = (p_1(t), p_2(t), q_1(t), q_2(t))$ cuts the (p_2, q_2) plane.

where f(x) is a scalar funciton. We only consider the case in which the iterates of f(x), that is, $x_0, x_1 = f(x_0)$, $x_2 = f[f(x_0)]$, etc., are bounded, $p < x_n < q$. Let us consider the following one-dimensional maps.

a) $F_1(x) = a(1-2|x-\frac{1}{2}|)$, $0 < a \leq 1$ (1.7a)

b) $F_2(x) = 2x \bmod 1$ (1.8)

c) $F_3(x) = 4bx(1-x)$, $0 < b \leq 1$ (1.9)

where a and b are constants. For $0 < a < 1$, $0 < b < 1$ both F_1 and F_3 map the interval 0 to 1 into itself. All the above functions are non-invertible, since given x_{n+1}, one cannot solve $x_{n+1} = F(x_n)$ for x_n.

a) $F_1 = a(1-2/x-\frac{1}{2}/)$. There are essentially two cases of interest, $0 < a < \frac{1}{2}$ and $\frac{1}{2} < a \leq 1$.

For $0 < a < \frac{1}{2}$, all iterates, x_n, converges to zero. For $\frac{1}{2} < a \leq 1$, the situation is not simple. For any initial x_0 between 0 and 1, the sequence after some iterations will be trapped in the interval $2a(1-a) < x < a$ through which it will wander chaotically, Fig. 1.7a. To illustrate this, consider the simple case a = 1 for which the chaotic interval becomes $0 < x < 1$. In this case we may consider the map to represent two steps: 1) uniform stretching o the interval 0 to 1 to twice its original length, and (2) a folding in half of the stretched interval so that it now has its original length, Fig. 1.7c.

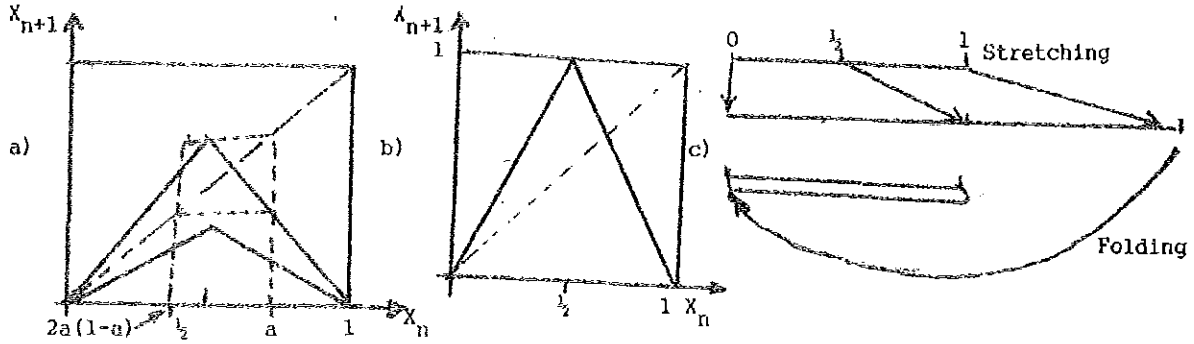

Fig.(1.7) a) Map of F_1 b) Map of F_1 for a = 1 c) Stretching and folding properties of F_1 for a = 1.

The stretching property leads to exponential separation of nearby points and hence, sensitive dependence on initial conditions. The folding property keeps the generated sequence bounded, but also causes the maps to be non-invertible, since it causes two different x_n points to be mapped into one x_{n+1} point [4]. Fig. 1.8 illustrates the stretching and folding properties of F_1 for a value of a less than one.

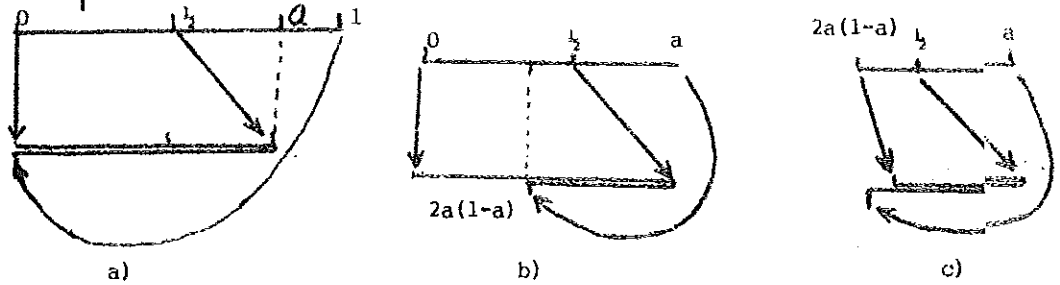

Fig. 1.8 Map of F_1 for $\frac{1}{2} < a < 1$.

a) mapping of the interval 0 to 1

b) 0 to a,

c) 2a(1-a) to a.

From Fig. 1.8b, we see that the interval 0 to 2a(1-a) is stretched but no points are folded back on to it. Thus, any point in $0 < x < 2a(1-a)$ will eventually leave that interval and never return. Thus the generated sequence is eventually trapped in $2a(1-a) < x < a$.

b) $F_2(x) = 2x \bmod 1$.

$$X_{n+1} = F_2(X_n) = 2x_n \bmod 1$$

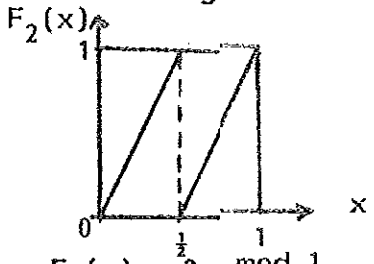

Fig. 1.9: $F_2(x) = 2x \bmod 1$

To one untutored in algorithmic art of generating Pseudo random numbers, forward iteration of the above first order difference equation appears guilelessly determinate [5]. In order to investigate the properties of this equation let us use binary representation of x_0.

$$X_o = \sum_{n=1}^{\infty} a_n 2^{-n} = (0,a_1a_2a_3\ldots)$$

where a_n has the value zero or unity. Then $X_1 = F_2(x_o) = (0,a_2a_3\ldots)$, $X_2 = F_2(X_1) = (0,a_3a_4\ldots)$, etc. Thus the action of F_2 on the binary representation of x_o is to move the decimal point sequentially to the right, each time dropping the integer part to the left of the decimal point. Such shifting property, Bernoulli shift, leads to the following points:

1. Sensitive dependence of the iterates of F_2 on the initial conditions. Choose $x_o = (0,a_1a_2\ldots a_n)$ and $x_o' = (0,a_1a_2\ldots a_n')$ which are very close to each other and differ by their n+h digit a_n. After (n-1) iterations their difference becomes amplified and their iterates $F_2^{n-1}(x_o) = (0,a_n)$ and $F_2^{n-1}(x_o') = (0,a_n')$ already differ in the first digit.

2. If we attach to $F_2^n(x_o)$ the symbol R or L depending on whether the iterate is contained in the right or left part of the interval, then we can find an x_o such that the sequence of iterates $F_2^n(x_o)$ has the same random properties as successive tosses of a coin.

3. It shows also the mechanism by which ergodicity emerges in a deterministic system. The image of an 'arbitrary' irrational number $x_o \in [0,1]$, $F_2^r(x_o)$ approach any chosen point x in the unit interal an infinite number of times. That is the system behaves ergodically, unless x_o is not an element of a set of measure zero.

Stretching and folding properties can also be demonstrated for this map: If $X_0 < \frac{1}{2}$, X_0 becomes stretched after each iteration by a factor of 2. But for $n > n_o$ with $2^{n_o}X_o \geq 1$ folding takes place as shown in fig. 1.10.

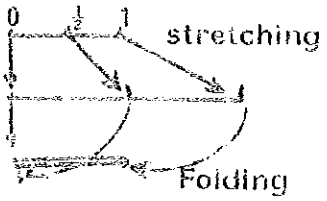

Fig. 1.10: Stretching and folding property of $F_2(x)$

Thus from the above two examples and other similar maps we conclude that the two basic ingredients for the generation of deterministic chaos are stretching and backfolding property of the map. That is in order for a one dimensional map to exhibit chaotic behavior, it must be non invertible.

c) $F_3(x) = 4bx(1-x)$, $0 < b \leq 1$. [6],[7],[8],... This map has a very rich behavior and some practical importance in explaining some dynamical systems. It shows regular and chaotic motion for a certain range of b. Before we procced to this map, we will characterize quantitatively whether a given signal is chaotic or not.

1.3 Characterization of Chaotic Motion

We have three quantitative measures for chaotic motion which is generated by one-dimensional maps [6]. These are the Liapunov exponent, Invariant measure, and correlation function.

1.3.1 Liapunov Exponent

For a map $X_{n+1} = f(x_n)$ which shows chaotic motion adjacent initial points become separated. The Liapunov exponent measures this exponential separation. The Liapunov exponent, $\lambda(x_o)$, is defined as:

$$\lambda(x_o) = \lim_{N\to\infty} \frac{1}{N} \ln\left|\frac{d\, f^N(x_o)}{d\, x_o}\right| \qquad (1.10)$$

This can be illustrated graphically as:

$$x_o \quad x_o+\varepsilon \xrightarrow{\text{After N iterations}} f^N(x_o) \quad f^N(x_o+\varepsilon) \qquad \varepsilon\, e^{N\lambda}$$

As the limit $\varepsilon \to 0$, $N\to\infty$ we obtain the correct expression for $\lambda(x_o)$, as in Eq. (1.10).

Example: Triangular map $f(x) = a(1-2/x-\frac{1}{2}/)$, $0 < a \leq 1$ for $a = 1$

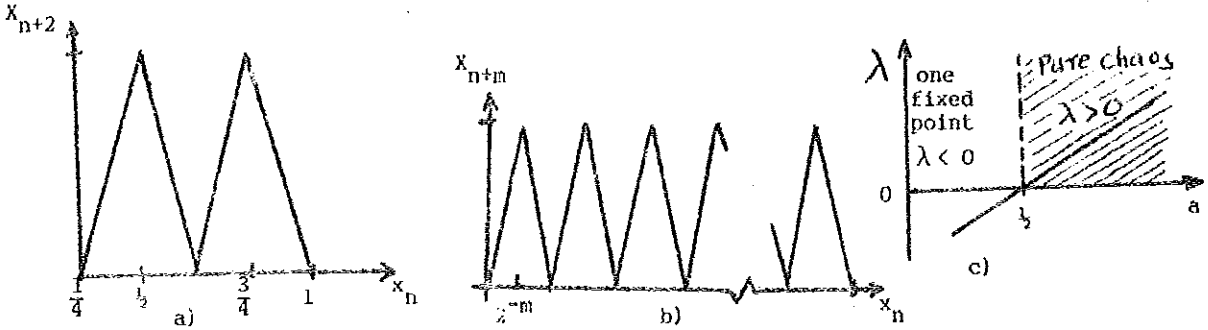

Fig. 1.12: a) $X_{n+2} = f^2(x_n)$ b) generalization of (a) to m itrations of $f(x_n)$.

c) The Liapunov exponent for the triangular map as a function of a in the vicinity of $a = \frac{1}{2}$.

The Liapunov exponent for the above map is $\lambda(x_o) = \log 2 > 0$. That is initial points separate exponentially. For any value of a, $\lambda = \ln 2a$. If $a > \frac{1}{2}$, we have chaotic motion; for $a < \frac{1}{2}$, no exponential separation of initial points and hence no Chaos, Fig. 1.12c.

1.3.2 The Invariant Measure

The invariant measure $\rho(x)$, determines the density of iterates of a unimodular map

$$x_{n+1} = f(x_n), \quad x_n \in [0,1], \; n = 0,1,2,\ldots \qquad (1.11)$$

over the unit interval and is defined as

$$\rho(x) = \lim_{N\to\infty} \frac{1}{N} \sum_{i=0}^{N} \delta[x-f^i(x_o)]. \qquad (1.12)$$

This formal expression allows us to write "time averages" over a function g(x) as averages over the invarieant measure.

$$\lim_{N\to\infty} \frac{1}{N} \sum_{i=0}^{N} g(x_i) = \lim_{N\to\infty} \frac{1}{N} \sum_{i=0}^{N} g[f^i(x_o)] = \int_o^1 dx\ \rho(x)g(x) \qquad (1.13)$$

It can be shown that $\rho(x)$ can be calculated from the following equation:

$$\rho(y) = \int_0^1 dx\ \delta[y-f(x)]\ \rho(x) \qquad (1.14)$$

The question wheather $\rho(x)$ is unique, can only be answered by looking to the solutions to (1.14) for special maps f(x). Let us consider the triangular map for a = 1:

$$F_1(x) = \begin{cases} 2x, & x \leq \frac{1}{2} \\ 2(1-x), & x > \frac{1}{2} \end{cases}$$

In this case eqn. (1.14) becomes:

$$\rho(x) = \tfrac{1}{2}\left[\rho\left(\frac{x}{2}\right) + \rho\left(1 - \frac{x}{2}\right)\right] \qquad (1.15)$$

which has the obvious normalised solution $\rho(x) = 1$.

This means that for the triangular map at a = 1 the chaotic sequence of iterates x_o, $f(x_o)$, $f^2(x_o)$,... uniformly covers the interval [0,1], and the system is ergodic.

1.3.3 Correlation Function

The correlation function C(m) for a map

$$X_{n+1} = f(x_n) \quad , \quad x_n \in [0,1], \; n = 0,1,2,\ldots$$

is defined by

$$C(m) = \lim_{N\to\infty} \frac{1}{N} \sum_{i=0}^{N} \hat{x}_{i+m}\, \hat{x}_i \tag{1.16}$$

where $\hat{x}_i = f^i(x_o) - \bar{x}$; $\bar{x} = \lim_{N\to\infty} \frac{1}{N} \sum_{i=0}^{N} f^i(x_o)$ (1.17)

It tells us, how much the deviations of the iterates from their average value, $\hat{x}_i = x_i - \bar{x}$, that are m steps apart (x_i and x_{i+m}) know about each other, on the average.

If the invariant measure $\rho(x)$ for a given map f(x) is known, C(m) can be written in the following form.

$$C(m) = \int_0^1 dx\, \rho(x) x\, f^m(x) - \left[\int_0^1 dx\, \rho(x) x\right]^2 \tag{1.18}$$

If we apply this equation for the triangular map, a = 1, one can show that

$$C(m) = \int_0^1 dx\, x\, F_1^m(x) - \left[\int_0^1 dx\, x\right]^2$$

$$= \int_{-\frac{1}{2}}^{\frac{1}{2}} dy\, y\, F_1^m(y+\tfrac{1}{2}) + \tfrac{1}{2} \int_{-\frac{1}{2}}^{\frac{1}{2}} dy\, F_1^m(y+\tfrac{1}{2}) - \frac{1}{4}$$

$$= \frac{1}{12} \delta_{m,o} \tag{1.20}$$

C(m) is delta-correlated.

To summarize, we have found for a general one dimensional map that a sequence $x_o, f(x_o), \ldots, f^n(x_o) \ldots$ can be characterized (a) by a Liapunov exponent which tells us how adjacent points become separated under the action of f; (b) by the invariant density which serves as a measure of how the iterates become distributed over the unit interval; (c) by the correlation function C(m) which measures the correlations between iterates that are m steps apart.

2. Universal Properties of Quadratic Maps

Some very simple schemes which produce chaos behave identically to some of the chaotic aspects of natural phenomena. We have now convincing evidence that the problem of how a fluid changes over from smooth to turbulent flow can be solved through its relation to the behavior of simple quadratic map under this chapter. Other natural problems that can be treated in the same way are the behavior of population from generation to generation and the noisness of a large variety of mechanical, electrical and chemical oscillators [1],[7],[8].

The feature common to these phenomena is that, as some external parameter is varied, the behavior of the system changes from simple to erratic. More specifically, for some range of the parameter values, the system exhibits an orderly periodic behavior; say with period T. Beyond this range it needs a period of 2T to repeat itself. For the next range of the parameter it required 4T to reproduce itself. This process of successivie period doubling recurs continually until, at a certain value of the parameter, it has doubled ad infinitum, so that the behavior is no longer periodic. Period doubling is then a characteristic route for a system to follow as it changes over from simple periodic to complex aperiodic motion. In the limit of aperiodic behavior, there is a unique and hence universal solution common to all systems undergoing period doubling. The sequence

$$\frac{b_{n+1} - b_n}{b_{n+2} - b_{n+1}}$$

, where b_n is the value of the parameter at which its period doubles for the nth time will reach a special value, the irrational

number, $\delta = 4.669...$ [7]. Delta, δ , seems to be a natural constant. This number, Feigenbaum's constant, is as characteristic for the period doubling scenario as the number π for the geometry of a circle [9]. This definite number must appear as a natural rate in Oscillators, populations, fluids, and all systems undergoing a peiod doubling route. Therefore, it is sufficient to study the simplest system exhibiting this phenomena to comprehend the general complex one.

2.1 The Logistic Map

In this section we study the logistic map

$$X_{n+1} = 4\, b\, X_n(1-X_n), \quad X_n \in [0,1], \quad n = 0,1,2,... \qquad (2.1)$$

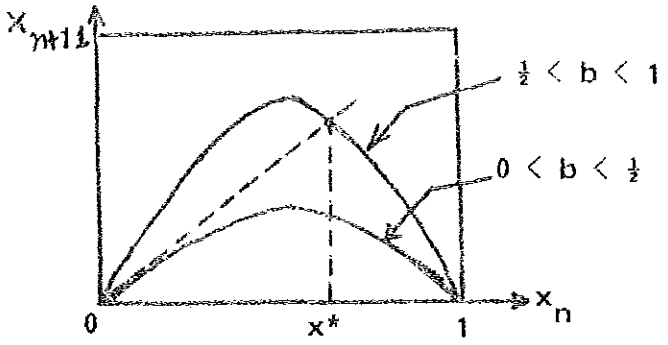

Fig. 2.1 A quadratic map on the unit interval

As found by different people and Feignbaum (1978), the iterates $x_0, x_1, x_2, ...$ of Eqn (2.1) display, as a function of the external parameter b, a rather complicated behavior which becomes chaotic at large b's, Fig. 2.2.

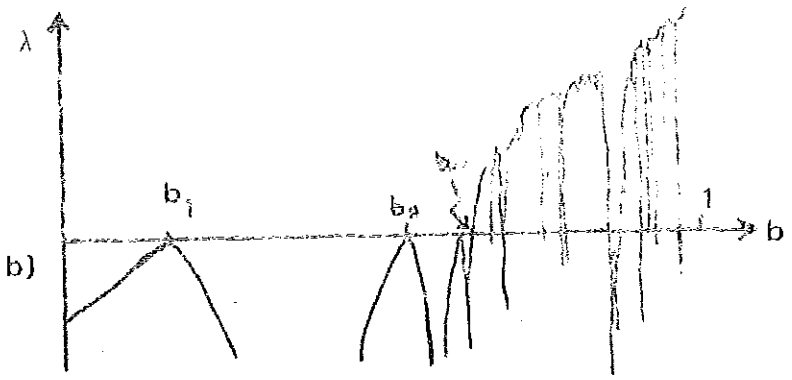

Fig. 2.2: Liapunov exponent for the logistic map

One has to note that chaotic behavior is not tied to the special form of the logistic map. Feignbaum has shown that the route to chaos which is found in the Logistic map, "the Feignbaum route" [10], occurs (with certain restrictions) in all first order difference equations $X_{n+1} = f(x_n)$ in which $f(x_n)$ has only a single maximum in the unit interval $0 \leq x_n \leq 1$. Because the conditions for the appearance of the Feigenbeum route are rather weak this route has been observed experimentally in many nonlinear systems.

Let us now make a direct onslought against equation (2.1) to see what it possesses. We want to know the behavior of the system after many iterations. As you can guess, higher iterates of f rapidly becomes very complicated. One way this complication can be prevented is to have the first iterate of x_o be precisely x_o itself. Such a self reproducing point is called a fixed point of f. The sequence of iterates is then $x_o, x_o, x_o, \ldots$ so that the behavior is static or if viewd as periodic, it has period 1.

Thus the fixed points, for $f(x) = 4bx(1-x)$ are $x=0$ and

$x^* = 1 - \frac{1}{4b}$.

2.1.1 Mechanism of Peirod Doubling (Pitchfork Bifurcation)

The Pitchfork bifurcation provides the mechanisms by which successive fixed points doubles [6],[7],[8]. To understand this mechanism we must state a condition for a fixed point to be stable or unstable to small perturbations. Let $\bar{x}$ be a fixed point, $\bar{x} = F(\bar{x})$, and consider a perturbation from it, $x_n = \bar{x} + \delta_n$. From $x_{n+1} = f(x_n)$, $\bar{x} + \delta_{n+1} = F(\bar{x}+\delta_n)$. For δ_n small, we can use Taylor's expansion for $F(\bar{x}+\delta_n)$

$$F(\bar{x}+\delta_n) = F(\bar{x}) + F'(\bar{x})\delta_n = \bar{x} + F'(\bar{x})\,\delta_n,$$

from which we obtain

$$\frac{\delta_{n+1}}{\delta_n} = F'(\bar{x}). \qquad (2.2)$$

Thus if $|F'(\bar{x})| > 1$, images under F of points near $\bar{x}$ successively move further away from it, and $\bar{x}$ is unstable. For $|F'(\bar{x})| < 1$, points near $\bar{x}$ converge to it, and $\bar{x}$ is stable.

Now we must ask for what values of b are the fixed points attracting?

$f'(x) = 4b(1-2x)$ so that it's value at $x = 0$, $x^* = 1 - \frac{1}{4b}$, are $f'(0) = 4b$, and $f'(x^*) = 2-4b$. We can show that for $0 < b < \frac{1}{4}$, only $x = 0$ is stable, at $b = \frac{1}{4}$, $f'(x^*) = 1$. For $\frac{1}{4} < b < \frac{3}{4}$, $x = 0$ is unstable and x^* is stable, while at $b = \frac{3}{4}$, $f'(x^*) = -1$ and x^* also become unstable. Thus, for $0 < b < \frac{3}{4}$, the eventual behavior is known. See Fig. 2.3.

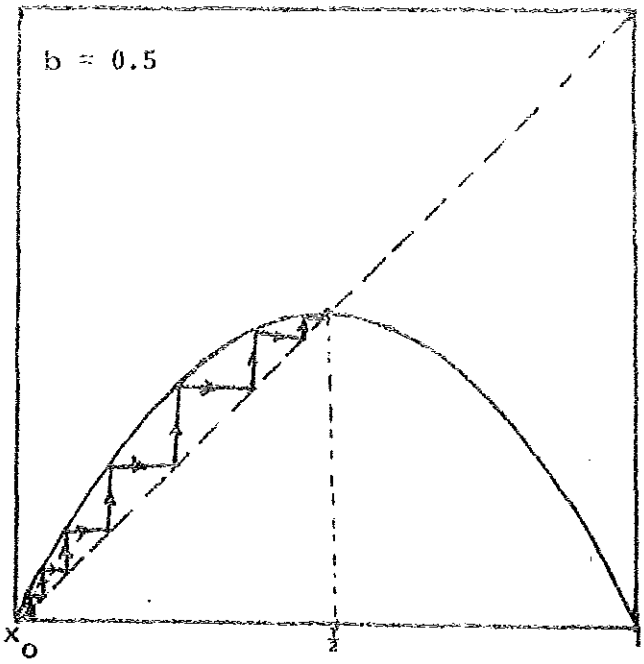

Fig. 2.3: Iterates of x_0 for b = 0.5

What happens to the system when b is in the range $\frac{3}{4} < b < 1$, where there are no attracting (stable) fixed points? We will see that as b increases slightly beyond $b = \frac{3}{4}$, f undergoes period doubling. That is instead of having a stable cycle of period 1 corresponding to one fixed point, the system has a stable cycle of period 2; that is the cycle contains two points. Since this two points are fixed points of the function f^2 and since stability is determined by the slop of a function at its fixed points, we must now focus on f^2. First we examine agraph of f^2 at b just below $\frac{3}{4}$. Fig 2.4a and b show f and f^2, respectively, at b = 0.7.

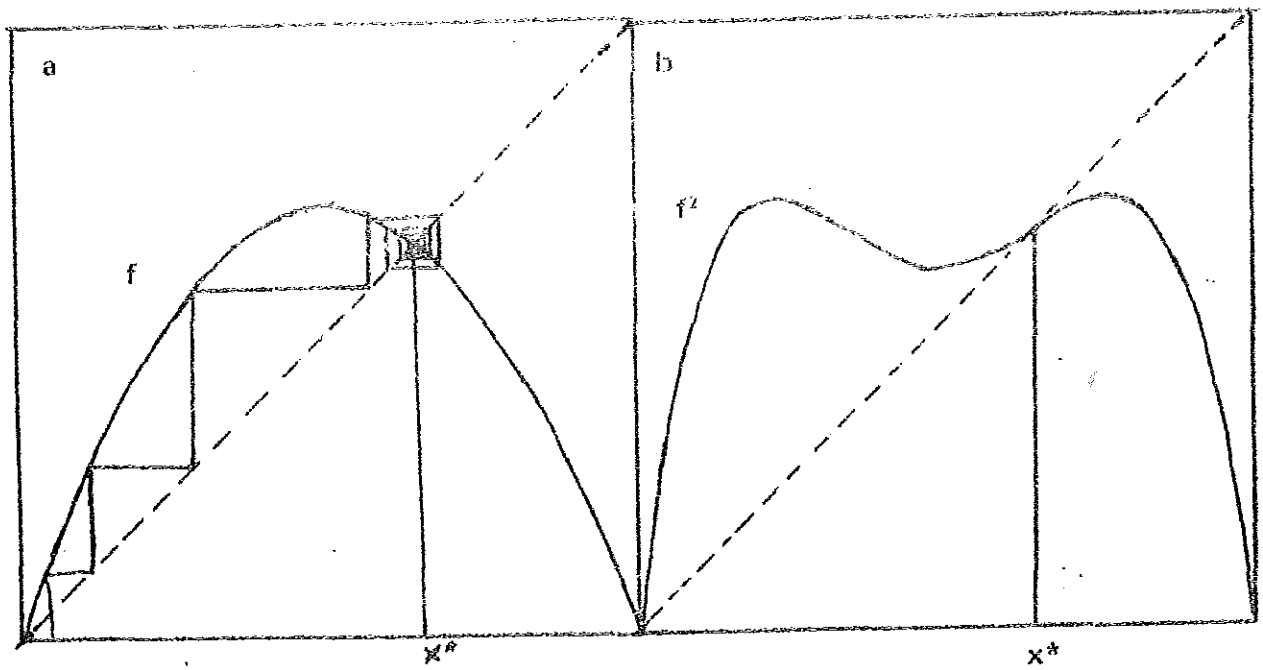

Fig. 2.4 b = 0.7. x^* is the stable fixed point.

To understand, Fig. 2.4b, observe first that, since f is symmetric about its maximum at $x = \frac{1}{2}$, f^2 is also symmetric about its maximum at $x = \frac{1}{2}$. Also, f^2 must have a fixed point whenever f does becaues the second iterate of a fixed point is still that fixed point. The main ingredient that determines the period - doubling behavior of f as b increases is the relationship of the slop of f^2 to the slop of f. This relationship is a consequence of the chain rule. it can easily be shown that

$$\frac{d}{dx} f^2(x_0) = f'(x_0)\, f'(x_1) \qquad (2.3)$$

where $x_1 = f(x_0)$. similarly

$$\frac{d}{dx}[f^n(x_0)] = f'(x_0)\, f'(x_1) \ldots f'(x_{n-1}) \qquad (2.4)$$

A simple result that determines period doubling. If we start at a fixed point of f and apply Eq. (2.3) to $x_0 = x^*$, so that $x_1 = x^*$, then

$$f^{2\prime}(x^*) = f'(x^*) \cdot f'(x^*) = \left|f'(x^*)\right|^2 \qquad (2.5)$$

Since at b = 0.7, $\left|f'(x)\right| < 1$, it follows from the above equation (2.5) that $0 < f^{2\prime}(x^*) < 1$.

To turn to Fig. 2.4, as b $\longrightarrow \frac{3}{4}$ and the maximum value of f increases to $\frac{3}{4}$, $f'(x^*) \to -1$ and $f^{2\prime}(x^*) > 1$, so that f^2 must develop two new fixed points beyond those of f; that is, f^2 will cross y = x at two more points. This transition is depicited in Fig. 2.5 a and b for f and f^2, respectively, at b = 0.75, and

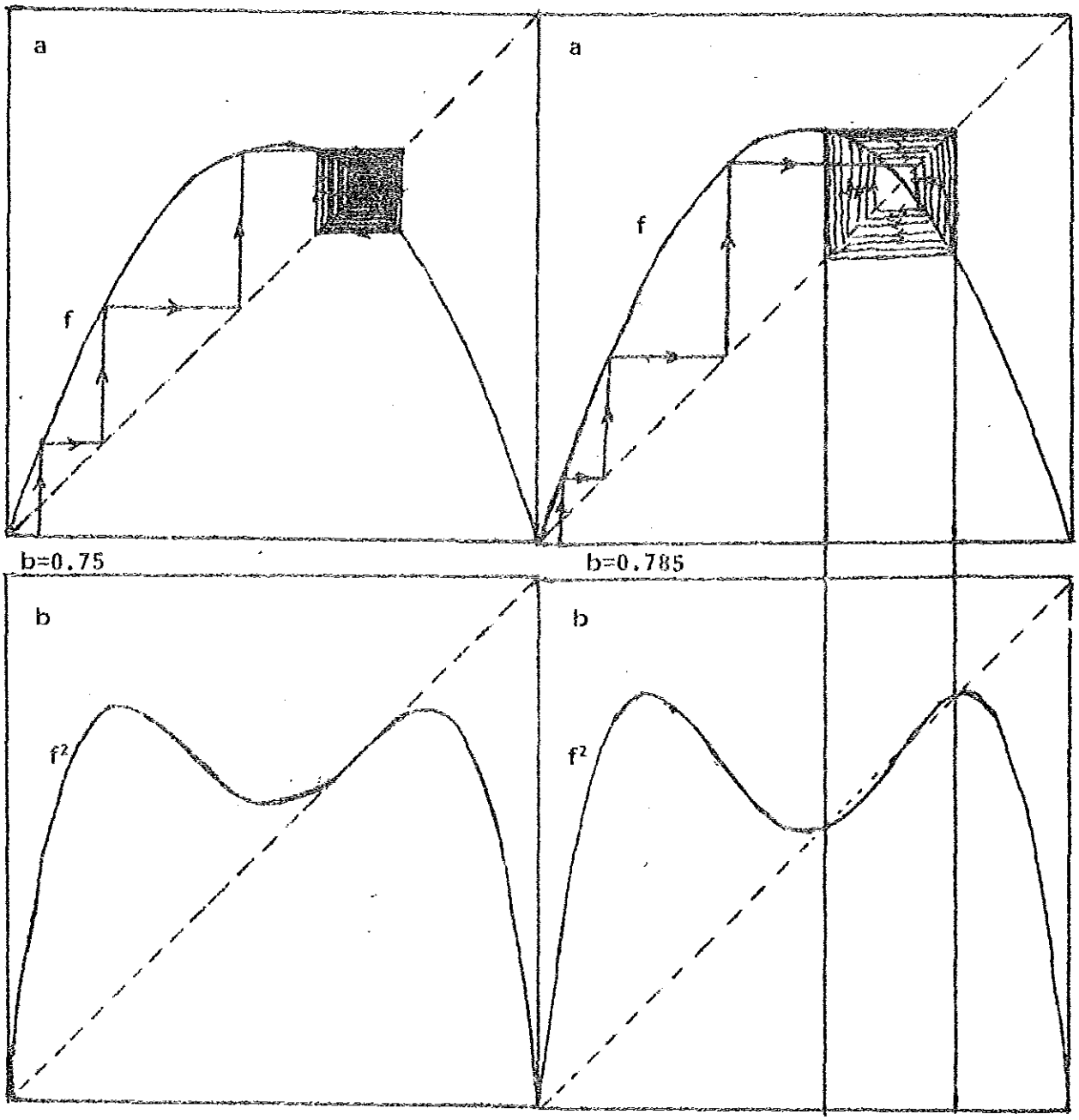

Fig. 2.5: f and f^2 for b = 0.75

Fig. 2.6: f and f^2 for b = 0.785

similarly in Fig. 2.6 a and b at b = 0.785. Since x_1^* and x_2^*, the new fixed points of f^2, are not fixed points of f, it must be that f sends one into the other:

$$x_1^* = f(x_2^*) \text{ and } x_2^* = f(x_1^*). \qquad (2.6)$$

values of x which recur every second iteration, in series $x_1^*, x_2^*, x_1^*, x_2^*, \ldots$ are fixed points of f^2. Such a pair of points, termed a 2-cycle or an attractor of period 2 is depicited by the limiting unwinding circulating square in Fig. 2.6 a.

Thus, we have observed for the quadratic map the first period doubling as the parameter b has increased.

As b is increased further, the minimum at $x = \frac{1}{2}$ will drop as the slope of f^2 through the fixed point of f increases. At some value of b, denoted by b', $x = \frac{1}{2}$ will become a fixed point of f^2. Figures 2.7 a and b depicit the situation that occurs at $b = b'$.

As we increase b further, the minimum drops still lower, so that both x_1^* and x_2^* have negative slopes. At some paramter value denoted by b_2 the slope at both x_1^* and x_2^* become equal to -1. Thus the same situation has developed for f^2 as developed for f at $b_1 = \frac{3}{4}$. This transition case is depicited in Figs. 2.8 a and b. Accordingly, just as the fixed point of f at b_1 issued into being a 2-cycle, so too does each fixed point of f^2 at b_2 create a 2-cycle, which in turn is a 4-cycle of f. That is, when x_1^*, x_2^* cycle looses stability, a stable four-point periodic cycle simultaneously apears, i.e., $y_1^*, y_2^*, y_3^*, y_4^*, y_1^*, y_2^*, \ldots$ see Fig. 2.10. Thus, we have now met the second period doubling. Fig. 2.8 shows this situation for f and f^2, respectivelly.

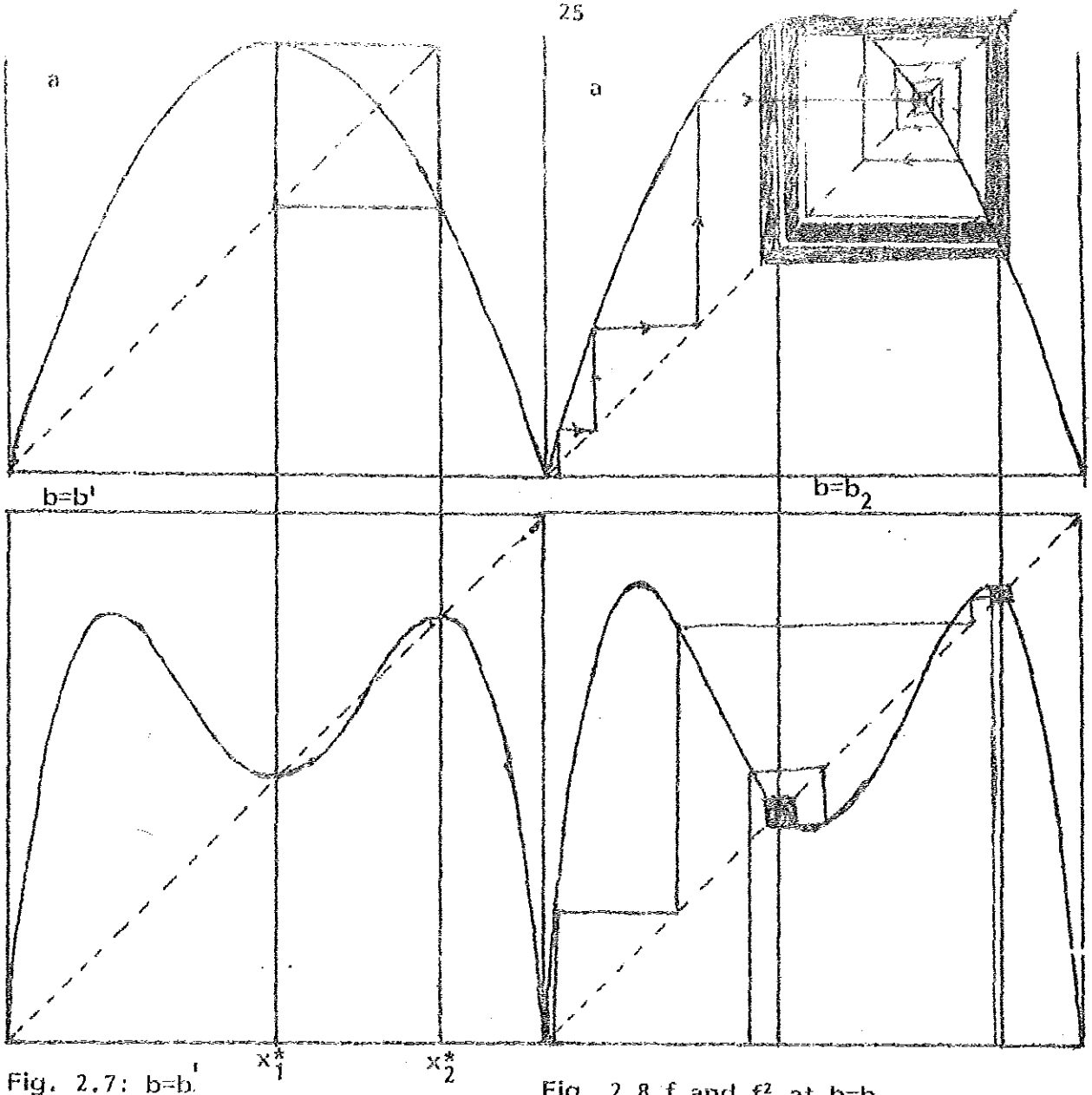

Fig. 2.7: $b=b'$

Fig. 2.8 f and f^2 at $b=b_2$

When b increases further, the maximum of f^4 at $x = \frac{1}{2}$ now moves up, developing a fixed point with negative slope. Finally, at b_3 when the slope of this fixed point is again -1, each fixed point will split into a pair giving rise to 8 cycle, which is now stable, etc. see Fig. 2.9. This period doubling continues ad infinitium upto a certain value of b, b_∞.

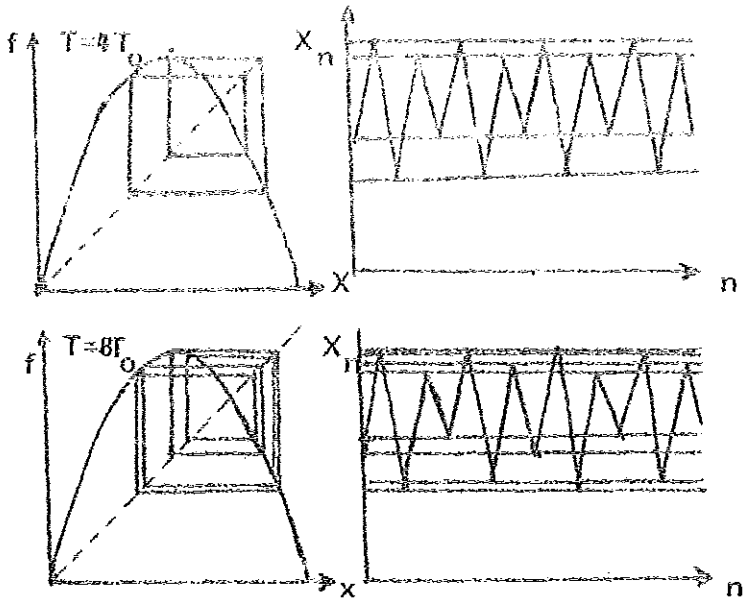

Fig. 2.9: Iteration of the map f for four and eight cycles.

The band of b values over which a given 2^n-point cycle is stable de geometrically with n, so that

$$\delta_n = \frac{b_{n+1} - b_n}{b_{n+2} - b_{n+1}} \xrightarrow[n\to\infty]{} \delta = 4.669201... \qquad (2.7)$$

where b_n is the value of b at the point where the 2^n-point cycle bifurcates (or looses stability) to a 2^{n+1}-point cycle [7]. In other words the parameter convergence is universal.

$$\frac{\Delta_i}{\Delta_{i+1}} \longrightarrow \delta = 4.6692...$$
for i large.

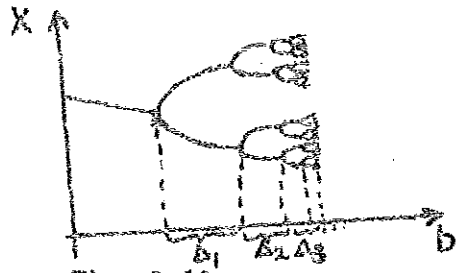

Fig. 2.10

In addition, the distance d_n of the point in a 2^n-cycle which are closest to $x = \frac{1}{2}$ have constant ratios:

$$\frac{d_n}{d_{n+1}} = -\alpha \qquad \text{for } n >> 1. \qquad (2.8)$$

That is the relative scale of successive branch splittings is univrsal, See Fig. 2.11.

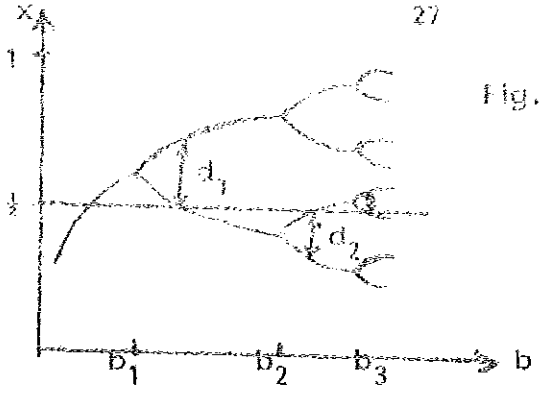

Fig. 2.11: Distances d_n of the fixed points closest to $x=\frac{1}{2}$ for superstable 2^n-cycles.

The constants α and δ, the Feigenbaum constants, have the values [7]:

$$\delta = 4.6692016091...$$

$$\alpha = 2.5029078750... \qquad (2.9)$$

2.1.2 Chaotic region, $b_\infty < b < 1$

In the chaotic region, $b_\infty < b < 1$, where the Liapunov exponent, λ is mostely positive indicates chaotic behavior. The chaotic region is interrupted by b-windows with $\lambda < 0$ where the sequence $\{ f_b^n(x_o)\}$ is again periodic. This region has the following behavior [6]. [See Schuster, H.G; "Deterministic chaos"].

a) The chaotic intervals move together by inverse bifurcations until the iterates become distributed over the whole interval [0,1] at b=1.

b) The b-windows are characterized by periodic p-cycles (p = 3,5,6,...) with successive bifurcations $p, p.2^1, p.2^2$ etc. The correseponding b-values scale like eqn. (2.7) with the same δ.

c) In addition, period triplings $p.3^n$ and quadruplings $p.4^n$ etc. occur with different Feigenbaum constants $\bar{\delta}$, which are again universal.

2.1.3 Power Spectrum

We have stated that the physical significance of the scaling number α is that it sets the scale of trajectory splitting. But this is not good enough to make connection with experiments; the theory describes the splitting of the phase space trajectories, while experiementalists usually measure the power spectrum. Feignbaum has given a nice prediction of how the power spectrum evolves as a function of the parameter, Fig. 2.12 [10].

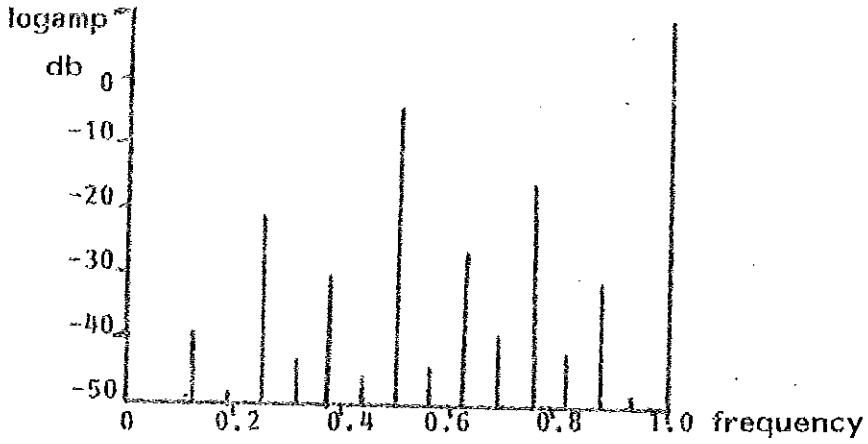

Fig. 2.12: Numerical predictions of the power spectrum

At each successive bifurcation a new frequency is born, and each subharmonic lies below the preceeding level by 8.17dB. The full details of this power spectrum however, cannot be observed experimentally because there will always be some external noise. This noise washes out the fine structure of the power spectrum.

We summarize the main finger prints of this route as follows:

1. There exists an infinite cascade of period doublings which lead to subharmonics in the power spectrum at frequencies $2^{-n}f_o$ where f_o is the basic frequency.

2. Each subharmonic lies below the preceeding level by a factor of 0.1525 (=8.17dB).
3. The controll parameter b scales for subsequent subharmonics n like $b_n - b_\infty \sim \delta^{-n}$.
4. External noise destroys the fine structure of the power spectrum.
5. The Poincare map of the system is one dimensional and shows a single quadratic maximum.

Let us add as a caveat that not all quadratic maps of the unit interval into itself display an infinite sequence of pitch fork bifurcations, but only those which have a negative Schwarzian derivative [6].

2.2 Experimental Support for Feigenbaum Route

This route to chaos is extremely well tested on numerical and physical grounds. The period doublings have by now been observed in most current low dimensional dynamical systems. Experiment with liquid helium have confirmed the predictions. In this section we will present a turbulence experiment and RCL-Oscillator.

2.2.1 Onset of Turbulence

We start by describing schematically the experiment of Lichaber[69] and Maurer, 1980 on the Benard cell. In this type of experiment a liqud contained in a small box is heated from the bottom Fig. 2.13a. The main points are (1) there is a controllable parameter, the Rayleigh number. (2) the system is dissipative. Whenever the Rayleigh number is increased, one waits for the transients to die out.

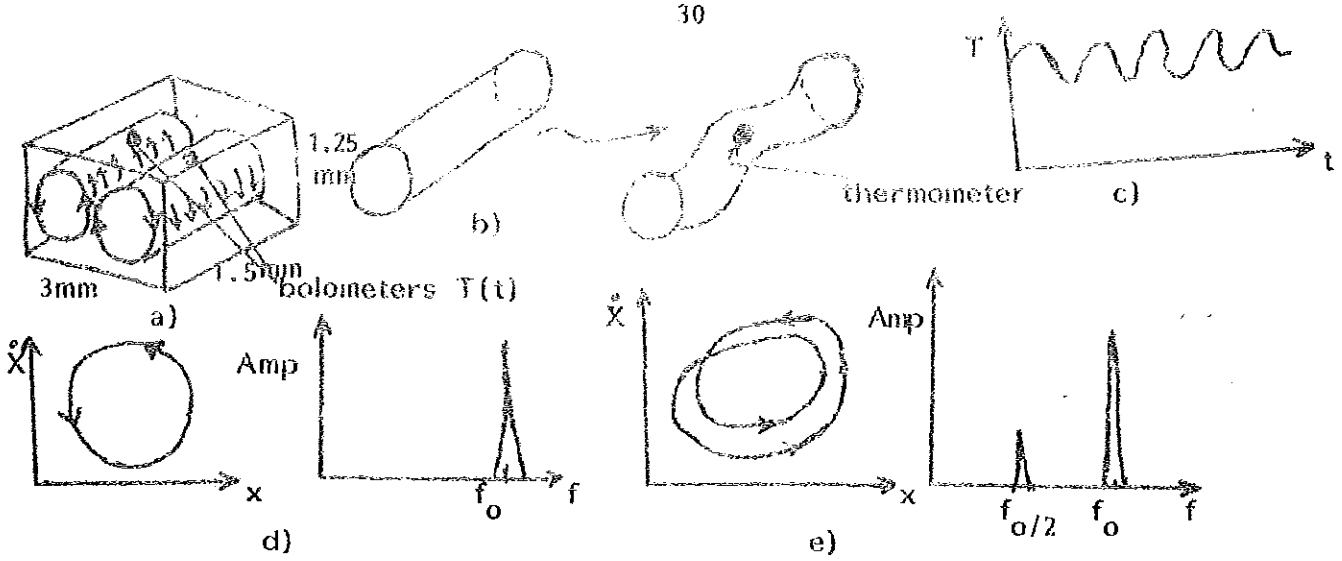

Fig. 2.13: Experiment of Lichober and Maurer, schematic description.

For small temperature differences there is a heat flow across the wall, but the liquid is static. At a critical temperature a convective flow sets in. The hot liquid rises in the middle, and the cold liquid flows down at the sides, and two convective rolls appear, Fig 2.13a..

As the temperature difference is increased further, a wave starts running along the roll. From this roll the position and the sidways velocity of the ridge can be measured with thermometer: one observes a sinusoidal, Fig. 2.13 b and c. The periodicity of this instability suggests two other ways of displaying the measurement: Phase space-sidways speed of the ridge, $\dot{x}$ versus position of the ridge, x and frequency spectrum - Amplitude, Amp, Versus frequency, f as in (d) and (e) [11].

Now, as the temperature difference is increased further we will observe Fig (2.13e). A new wave has appeared at half the original frequency. The trajectory closes itself after $2T_o$. As one, still, increases the temperature further the phase space undergoes a very fine splitting and the trajectory closes itself after $4T_o$. In addition, new frequencies $f_o/4$ and $3f_o/4$ are born. If the noise were not killing us, we would expect these splittings to continue. For a critical value of the Rayleigh number the periodicity of the system is $2^{\infty}T_o$, and the convective rolls have become turbulent.

Libchaber and Maurer (1980) [12] found the following properties of the Feigenbaum route in the Benard experiement with liquid helium, Fig. 2.14:

a) With increasing temperature difference there appear subharmonics of frequencies f/2, f/4, f/8 and f/16 where f is the basic frequency.

b) Subsequent subharmonics differ by about 10dB in qualitative agreement with theory.

Higher subharmonics are probably suppressed by external noise. Although these results leave little doubt that the Feignbaum route is involved, the explicit reduction of the hydrodynamic equations which describe the system to a one dimensional Poincare map with a single quadratic maximum has still not been demonstrated [6].

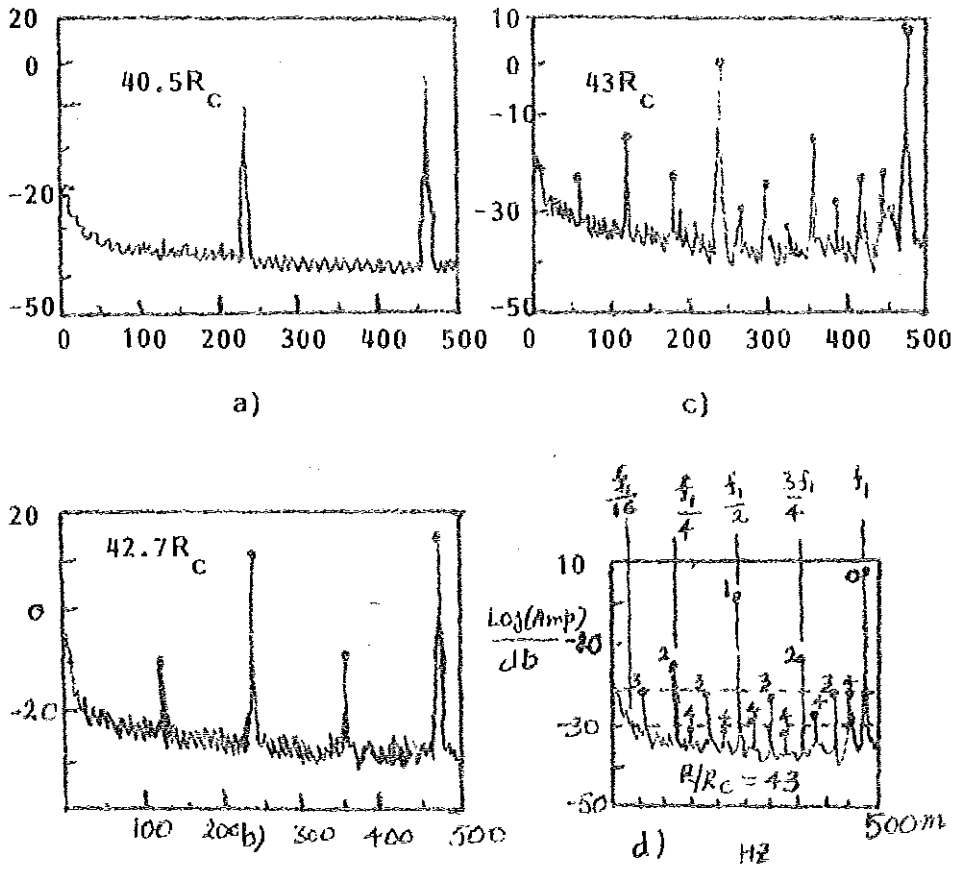

Fig. 2.14: (a-c) power spectrum with increasing Rayleigh number. d) the heights of the n-th subharmonics are compared with Feigen baum7s theory (horizontal line). (After Libchaber and Maurer,1980).

2.2.2 Nonlinear RCL-Oscillator

We have a nonlinear RCL-Oscillator shown in Fig. 2.15. The nonlinear element in this circuit is, according to Linsay (1981), [6] the capacitor diode, which leads to the following nonlinear relation between charge q and voltage V:

$$V(q) = \left[1 + \frac{V(q)}{0.6}\right]^{0.43} \frac{q}{C_0} \qquad (2.10)$$

The differntial equation for the time dependence of q is

$$L\ddot{q} + R\dot{q} + V(q) = V_0 \sin(2\pi f_1 t) \qquad (2.11)$$

Fig. 2.15 shows that for special value V_0 (which is proportional to the controll parameter b) the sequence of current signals $I_n = I(t_0 + nT)$, where the time $T = 1/f_1$, can indeed be generated from a one-dimensional map with a quadratic maximum.

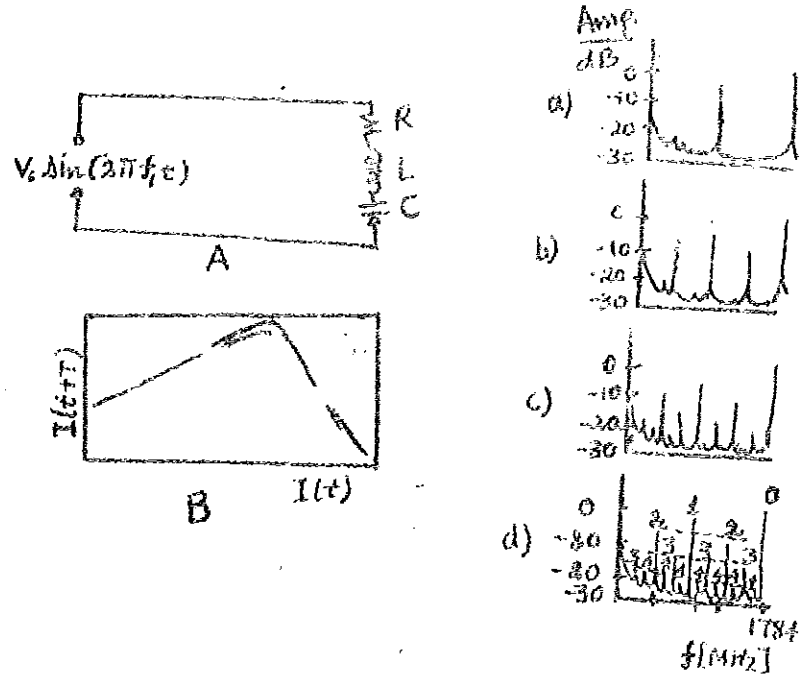

Measured value of the convergence rate

Subharmonic	$V_{threshold}$ (V)	δ_n
$f_{1/2}$	3.2±0.02	
		4.4±0.1
$f_{1/4}$	0.72±0.02	
		4.5±0.6
$f_{1/8}$	0.16±0.02	

C

Fig. 2.15 A) Circuit for the driven nonlinear RCL-Oscillator (B) The observed current I(t+T) Vs.I(t) yields a one-dimensional map with a single maximum (D) a-c subharmonics in the Power spectrum for increasing V_o; d:comparison with Feignbaum's theory.

The corresponding power spectrum exhibits-as expected - all the features of the bifurcation route and yields an estimate for δ which deviates by 10% from Feignbaum's asymptotic value.

3. The Intermittency Route to Chaos

Period-doubling are rather common, but they are by no means the only way in which a deterministic system can reach chaos. Intermittency is another type of chaotic behavior commonly observed in deterministic systems. It is characterized by long period of regular motion interrupted by short chaotic bursts. It has also been observed that the number of chaotic bursts increases with an external paramter, which means that intermittency offers a continuous route from regular to chaotic motion.

3.1 Mechanisms for Intermittency

The intermittency route to chaos has been investigated in a pioneering study by Pomeau and Manneville (1979) [15]. They solved numerically the differential equation of the Lorenz model, eqn. (1.3):

$$\dot{X} = \sigma(X-Y)$$

$$\dot{Y} = -XZ + rX - Y$$

$$\dot{Z} = XY - bZ$$

and for the Y-component they found the behaviour shown in Fig. 3.1 [14].

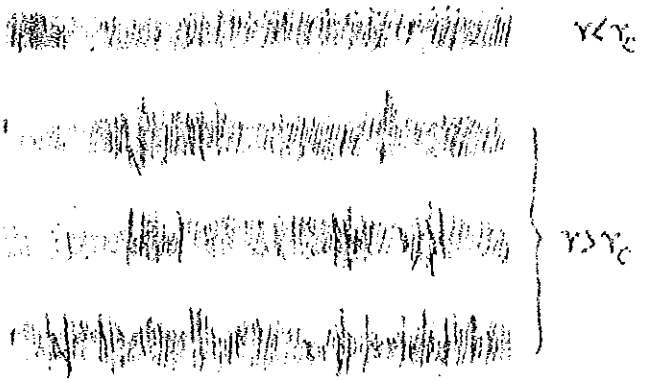

Fig. 3.1: Time plot of one coordinate in the Lorenze model (After Pomeau and Manneville (1980).

Pomeau and manneville gave the following interpretation for this behavior: the stable oscillations for $r < r_c$ correspond to a stable fixed point in the Poincare map. For $r > r_c$, this fixed point becomes unstable. Because there are essentially three ways in which a fixed point can lose its stability Pomeau and Manneville distinguished the three types of intermittency shown in Table

Table 1: Three Types of Intermittency

Type	Characteristic maps	Typical map $r < r_c$	$r > r_c$
I	$X_{n+1} = \varepsilon + X_n + uX_n^2$ $\varepsilon = r - r_c$	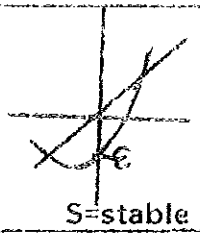	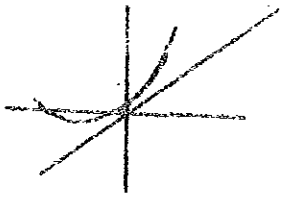
II	$r_{n+1} = (1+\varepsilon)r_n + ur_n^3$ $\theta_{n+1} = \theta_n + \Omega$		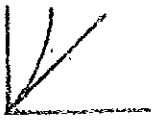
III	$X_{n+1} = -(1+\varepsilon)X_n - uX_n^3$		

Later, we will present the measurable characterisitc properties of different intermittency routes to chaos.

3.1.1 Type-I Intermittency

Figure 3.2 shows a Poincare map for the Lorenz model, after Pameau and Manneville [14] who plotted the values y_n where y(t) crossed the plane x = 0.

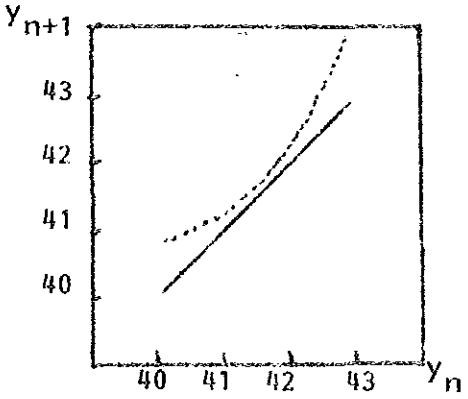

Fig. 3.2 Poincare map of the Lorenz model for r silightly above r_c = 166.

If fig. 3.2 is compared with table 1, it is seen that the Lorenz mode displays intermittency of type 1.

This transition to chaos is characterized by an inverse tangent bifurcation in which two fixed points (a stable and unstable one) merge as depicted in Fig. 3.3.

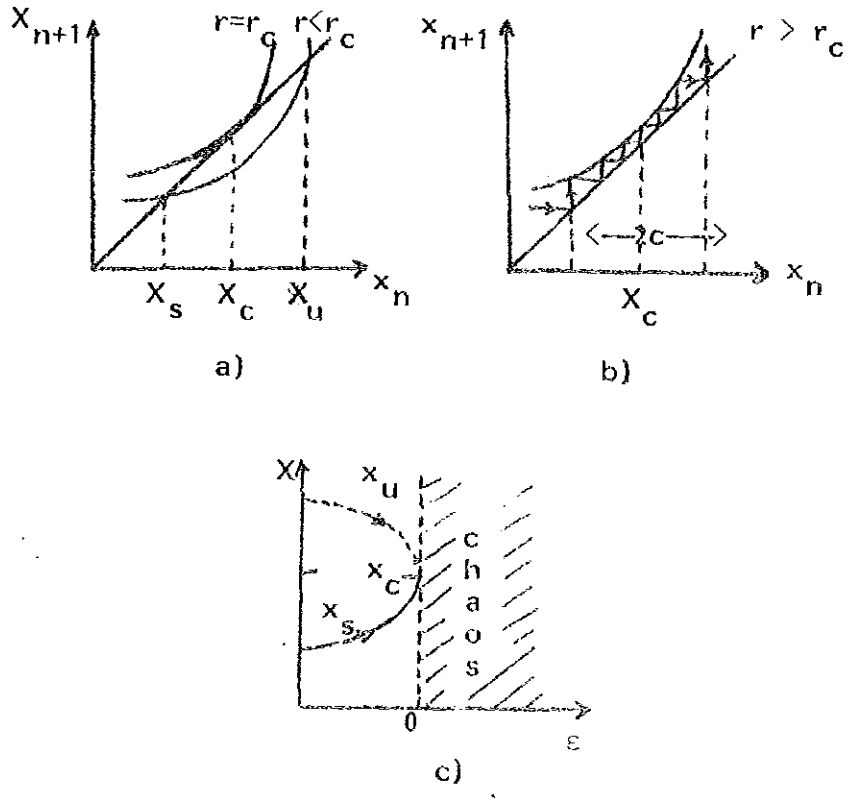

Fig. 3.3: Mechanism for type - I intermittency.

a) Poincare map for $r \leq r_c$ (b) Poincare map for $\varepsilon = r - r_c > 0$ (c) inverse tangent bifuration.

For $r > r_c$ the map has no stable fixed points. However, a sort of "memor of a fixed point is displayed since the motion of the trajectory slows down in the vicinity of x_c, and numerous iterations are required to move through

the narrow channel between the map and the bisector. This leads to the long laminar regions for values of r just above r_c in Fig. 3.1.

After the trajectory has left the channel, the motion becomes chaotic until reinjection into the vicinity of x_c starts a new regular phase. The theory of Pomeau and Manneville explains only the laminar motion but gives no information about the mechanism which generates chaos.

Another example for type-I intermittency appears in the logistic map

$$X_{n+1} = 4b\ X_n(1-X_n).$$

The iterates for b- values larger and smaller than $b_c = \frac{1}{4} + \frac{1}{\sqrt{2}}$ are shown in Fig. 3.4

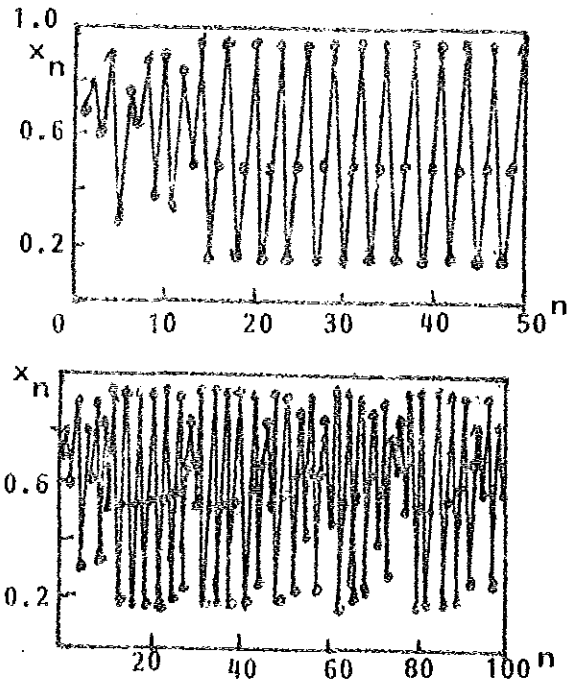

Fig. 3.4 Iterates of the logistic map starting from x = 0.7:

a) in stable three cycle region

$b_c - b = -0.005$

b) in the intermittent region

$b_c - b = 0.005$

There is a regular cycle of period three slightly above b_c, but below b_c laminar regions occur interrupted by chaos. Numerically it is found that at b_c this map exhibits a cycle of period three with subsequent bifurcations, i.e. there is a window as shown schematically in Fig. 3.5.

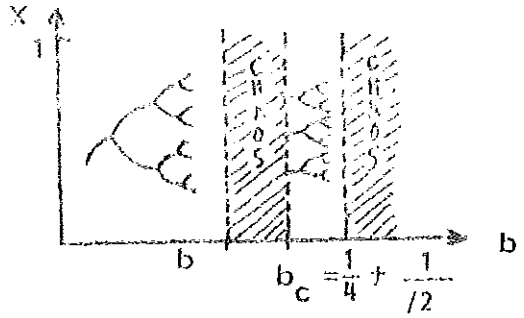

Fig. 3.5: Window with period three in the chaotic regime.

An explanation of this peculiar behavior follows from Fig. 3.6 which shows the third iterates of f(x) at $b = b_c$. There are fixed points which become unstable for $b < b_c$ and lead to intermittency of type I. Inverse tangent bifurcation, where a periodic orbit appears after a region of chaotic motion, only accounts for the generation of uneven number of fixed points from the logistic map [8].

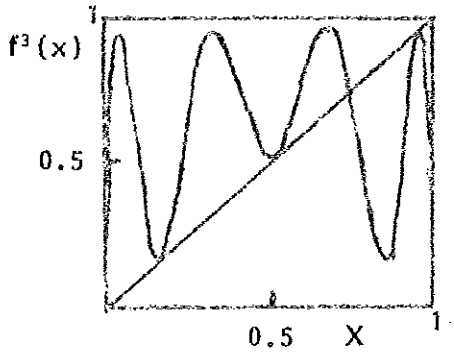

Fig. 3.6: The map for $f^3(x)$ at $b = b_c$

3.2. Summary of the Measurable Properties of Intermittency Route.

The average length $\langle \ell \rangle$ of a laminar region is given by using the renormalization group method and the results are listed for different types of intermittencies as shown in table 2. In addition the distribution of the laminar lengths, $P(\ell)$, and the respective laminar signal is given. This will help us to distinguish different types of intermittency.

Table 2: Characteristic Properties of Different Types of Intermittency

Type	Poincare map	Laminar signal	Laminar length $\langle \ell \rangle$ and Distribution $P(\ell)$
I	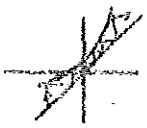	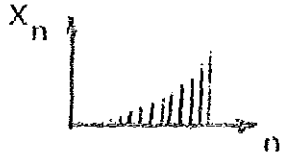 Increase monotonously.	$\langle \ell \rangle \sim \varepsilon^{-\frac{1}{2}}$ 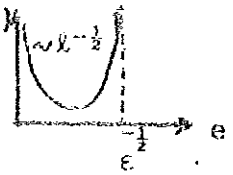
II		 spirals	$\langle \ell \rangle \sim \varepsilon^{-1}$ 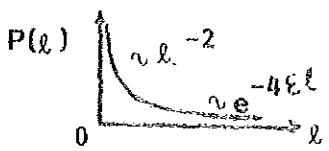
III	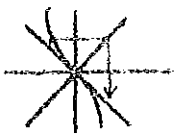	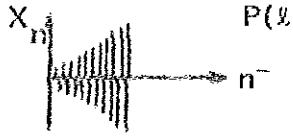 Alternates	$\langle \ell \rangle \sim \varepsilon^{-1}$ 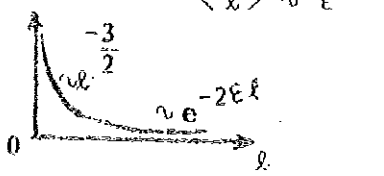

3.3 Experimental Evidence for Type-I Intermittency Route

In this route one should not look for power spectra, but rather at real-time measurements. Specifically, by making use of table 2 we can distinguish different types of intermittencies. We will present here three experiments for type I intermittency.

3.3.1 Benard Experiment

In this experiment the vertical velocity component, V_z, as a function of time is recorded as shown in Fig. 3.7. The signal shows a behavior which is typical for type-I intermittency [15].

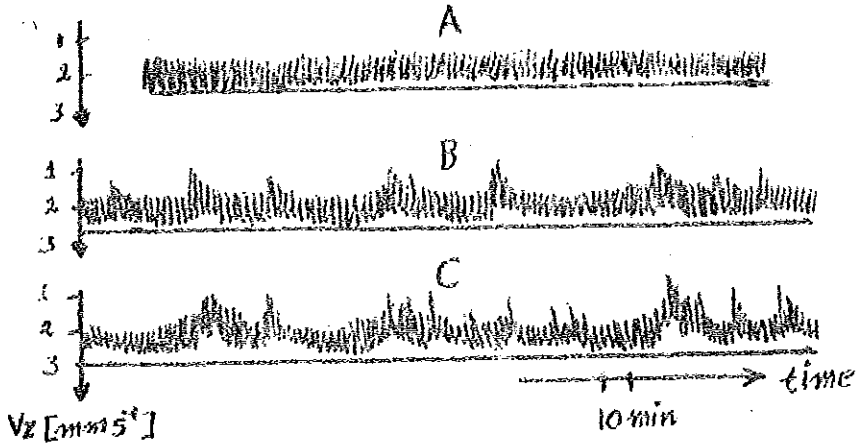

Fig. 3.7: Type-I intermittency for a Benard Experiment.
(After Berge, Dubois, Manneville, and Pomeau, 1980).

The vertical velocity component measured in the middle of Benard cell changes with increasing Rayleigh number from periodic motion A : $\frac{R_a}{R_a^c} = 270$ via intermittent motion B : $\frac{R_a}{R_q^c} = 300$ to chaos C : $\frac{R_a}{R_a^c} = 335$ where $R_a^c = 1700$.

3.3.2 Nonlinear RCL-Oscillator

The nonlinear RCL Oscillator, which we discussed in section 2.2.2, also displays the intermittency route. Type I intermittency is indicated in Fig. 3.8 by the Poincare map and the scaling behavior of the lengths of the laminar regions.

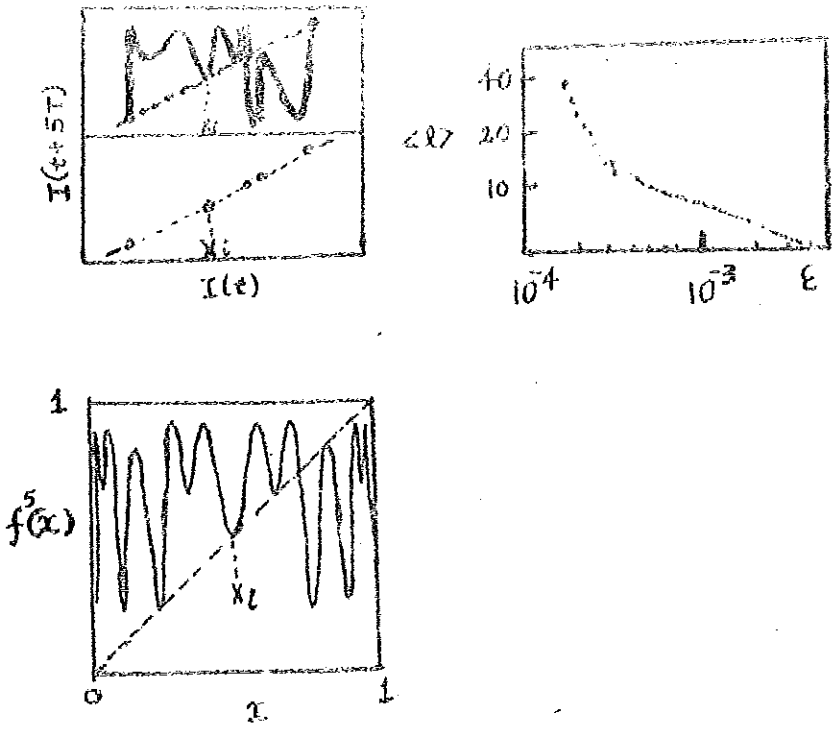

Fig. 3.8. Intermittency in the Nonlinear RCL-Oscillator:
a) I(t+5T) versus I(t) which corresponds to the fifth iterate of the logistic map at tangency which is shown in b). c) The measured averaged length for which the laminar regions scales like $\langle \ell \rangle \alpha\ \varepsilon^{-0.43}$ (where $\varepsilon \sim v_o - v_c$) is in reasonable good agreement with the prediction. (After Jiffries and Perez, 1982.)

3.3.3 Belousov-Zhabotinsky Reaction

This is another example which shows intermittent behavior. As we already mentioned, the concentration of the chemical species evolve according to nonlinear equaitons of chemical kinetics and this is enough to produce chaos. Fig. 3.9 shows type-I intermittency [16].

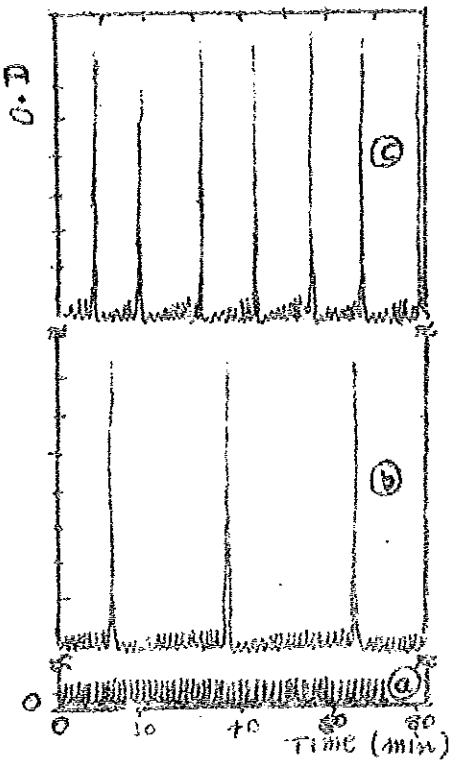

3.9: $[ce^{4+}]$ oscillations recorded as a function of time:

a) residence time 100 min; (b) residence time 76 min;
c) residence time 35 min.

When the mean residence time of chemicals in the reactor is 100 min., the optical density oscillates regularly. At higher fluxes (residence time 76 min.) the time changes in a specific manner: seemingly stable oscillations exist which are interrupted from time to time and at random by large peaks.

4. Strange Attractors in Dissipative Dynamical System

There are certain non-linear systems in which the trajectory becomes attracted to a bounded region of phase space in which the motion becomes chaotic. This particular region of phase space, in which initially close trajectories separate exponentially, are called strange attractors. Strange attractors are relatively abstract objects, but Computers give them some life, and draw pictures of them [1]. Strange attractors can produce print in the form of bagels, funnels, owlish eye and many other shapes. The dynamical systems which give rise to strange attractors are dissipative systems. In this section we will see some properties of strange attractors and we shall see how strange attractors are usful in explaining chaotic phenomena.

4.1 Introduction and Definition of a Strange Attractor

We will confine ourselves to dissipative systems which can be described eithere by flows or maps.

4.1.1 Dissipative Flows

These are described by a set of autonomous first-order differential equations,

$$\dot{\vec{X}} = \vec{F}(\vec{x};r) \quad ; \quad \vec{x} = (x_1, x_2, \ldots, x_d) \tag{4.1}$$

and the term dissipative means that an arbitrary volume element V enclosed by some surface S in phase space contracts. The surface S evolves by having each point on it follow an orbit generated by Eqn. (4.1). This yields by the divergence theorem

$$\frac{dV}{dt} = \int_V d^d x \left(\sum_{i=1}^{d} \frac{\partial F_i}{\partial x_i} \right) \tag{4.2}$$

and dissipative systmes are defined by $\frac{dV}{dt} < 0$.

Example: Lorenz model [2]. $V(t) = V(0)e^{-(\sigma+b+1)t}$ (4.3)

for $\sigma, b > 0$, the volume element contracts exponentially.

It can be shown that, for $r = 28, \sigma = 10$, $b = 8/3$, the trajectories generated by Lorenz model a) is attracted to a bounded region in phase space (b) the motion is erratic, i.e., it makes one loop to the right, then a few loops to the left, then to the right, etc. and (c) sensitive dependence of the trajectory on the initial conditions, i.e., if instead of (0,0,0) an adjacent initial condition, say (0,0,0.1), is chosen, then the new solution soon deviate from the old one, and the number of loops to the left and to the right would no longer be the same [1]. Fig. 4.1 shows a projection of the phase space orbit of the system into the YZ plane. The points labled C and C' are the steady convection equilibria points [2].

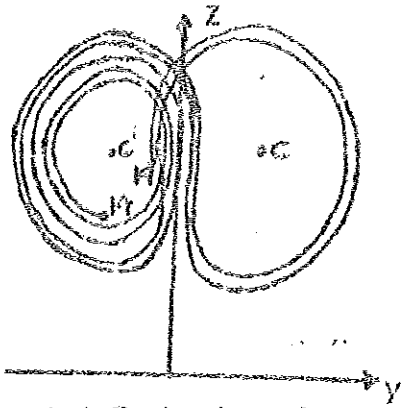

Fig. 4.1 Projection of an orbit for r=28 onto the YZ plane. The segment of the trajectory extending from iterations 1400 to 1900

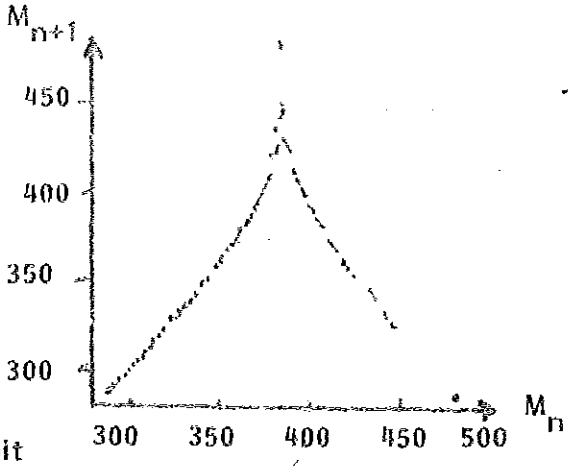

Fig. 4.2: Maxima V_s subsequent Maxima of Z occuring during 6000 iterations.

If we consider a map of the n+h maximum M_n of z versus M_{n+1}, we obtain a map which is, approximately a trinagular, Fig. 4.2. Furterhmore, $|dM_{n+1}/dM_n| > 1$, which is similar to the result for Eq. 1.7 with $a > \frac{1}{2}$. Thus, as for Eq. 1.4, we expect this one-dimensional map to generate a chaotic sequence.

The volume of this region contracts to zero implies the Lorenz system generates a set of points whose dimension is less than three. At first sight, one may think of the next lower integer dimension, two. However, this is forbidden by the Poincare -Bendixson theorem which states that there is no chaotic flow in a bounded region in two- dimensional space. The solution to this problem is that the set of points to which the trajector in the Lorenz system is attracted, the Lorenz attractor, has a Hausdorff dimension which lies between two and three, D = 2.06. Attractors which have noninteger dimensions are termed strange. The relevant definition of dimension is that due to Hausdorff [4], [17].

$$D = \lim_{\ell \to 0} \frac{\ln N(\ell)}{\ln\left(\frac{1}{\ell}\right)} \qquad (4.4)$$

where, if the set is a subset of m-dimensional ordinary space, then $N(\ell)$ is the number of m-dimensional cubes of side ℓ needed to cover the set. For $\ell \to 0$, Eq.(4.4) implies $N(\ell) \alpha\ \ell^{-D}$. This leads to a natural way to the concept of a strange attractor.

A strange attractor has the following qualitative properties [6]: (Read the article by J.P. Eckmann [10] for definition of a strange attractors)

a) It is an attractor, i.e., a bounded region of phase space to which all sufficiently close trajectories from the so-called basin of attraction are attracted asymptotically for long enough times. Furthermore the attractor should be indecomposable.

b) Sensitive dependence on the initial conditions. Despite the contraction in volume, lengths need not shrink in all directions, and points, which are arbitrarily close initially, become macroscopically separated at the attractor for sufficiently long times.

c) To describe a physical system, the attractor has to be structurally stable and generic. That is, a small change in the parameter of F in Eq. 4.1 changes the structure of the attractor contineously and the set of parameters for which Eq. 4.1 generates a strange attractor should not be of measure zero.

Upto now there is no generally accepted formal definition of strange attractors [10]. Therefore, it is not yet clear whether a fractal Hausdorff dimension follows from a) to c) or additionally required for a strange attractor.

A strange attractor arises typically when the flow contracts volume element in some directions and stretches it along the others. To remain confined to a bounded domain, the volume element is folded at the same time. This stretching and backfolding process produces a chaotic motion of the trajectory at the strange attractor.

Since the definition given above for strange attractors deals with properties of sets of points the concept of strange attractors applies equally well to dissipative maps.

4.1.2 Dissipative maps:

A map

$$\vec{x}\,(n+1) = \vec{G}\,[x_1(n),\ x_2(n),\ldots,x_d(n)] \qquad (4.5)$$

is called dissipative if it leads to a contraction of volume in phase space, i.e. if the absolute value of the Jacobian J, by which the volume element is multiplied after each iteration, is smaller than unity:

$$|J| = |\det(\frac{\partial G_i}{\partial x_j})| < 1 \qquad (4.6)$$

Because maps generate discrete points, the restriction imposed by the continuity of the flow for Poincare-Bendixson theorem, are lifted. Therefore maps can lead to strange attractors which also have dimensions less than two.

Let us consider two illustrative examples which are easier to visualize than the Lorenz system.

i) Baker's Transformation

The dissipative bakers transformation is given by

$$X_{n+1} = 2X_n \bmod 1$$

$$Y_{n+1} = \begin{cases} aY_n & , \quad 0 \leq x_n < \frac{1}{2} \\ \frac{1}{2}+aY_n & , \quad \frac{1}{2} \leq x_n < 1 \end{cases} \qquad (4.7)$$

where $a < \frac{1}{2}$

The first equation in Eq. 4.7 is the transformation for the Bernoulli shift. It has a Liapunov exponent, $\lambda_x = \log 2 > 0$, which is chaotic and makes the object from repeated applictions of this map to the unit square a strange attractor. The attractor is an infinite sequence of horizontal lines and its basin of attraction consists of all points within the unit square. In the y-direction, $\lambda_y = \log a > 0$, and lengths are contracted in this direction. The net effect is a volume contraction, as required for a dissipative map.

The Hausdorff dimension D_B of the strange attractor is the sum of the x and y dimensions. $D_x = 1$. In the y direction, D_y follows from its definition and equals to,

$$D_y = \log(\tfrac{1}{2})/\log a$$

$$D_B = 1 + D_y = 1 + \frac{\log 2}{|\log a|} \qquad (4.8)$$

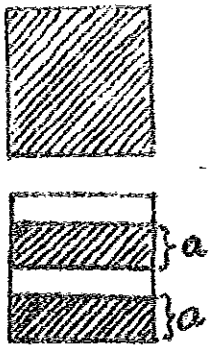

Fig. 4.3: Baker's transformation

ii) Henon Map

We now consider a mapping first studied by Henon (1976)

$$x_{n+1} = 1 - ax_n^2 + y_n$$
$$y_{n+1} = bx_n \qquad (4.9)$$

The Jacobian of this map is b, thus the map is an area contracting for $|b| < 1$. Given x_o, y_o we can compute x_n and y_n for $n = 1,2,\ldots,10,000$ for instance. Let us examine its iterates for $a = 1.4$, $b = 0.3$. Fig. 4.4a shows the result of an iteration with 10^4 steps. Some successive iterates have been numbered to illustrate their erratic movments on the attracotor. if the little square of Fig. 4.4a is magnified we get 4.4b. If the square of Fig. 4.4b is magnified, one would obtain a similar picture, and so on, each magnification revealing lines which were not previously visible. The Hausdorff dimension of the Henon attractors is $D(a=1.4, b=0.3) = 1.26$ [18].

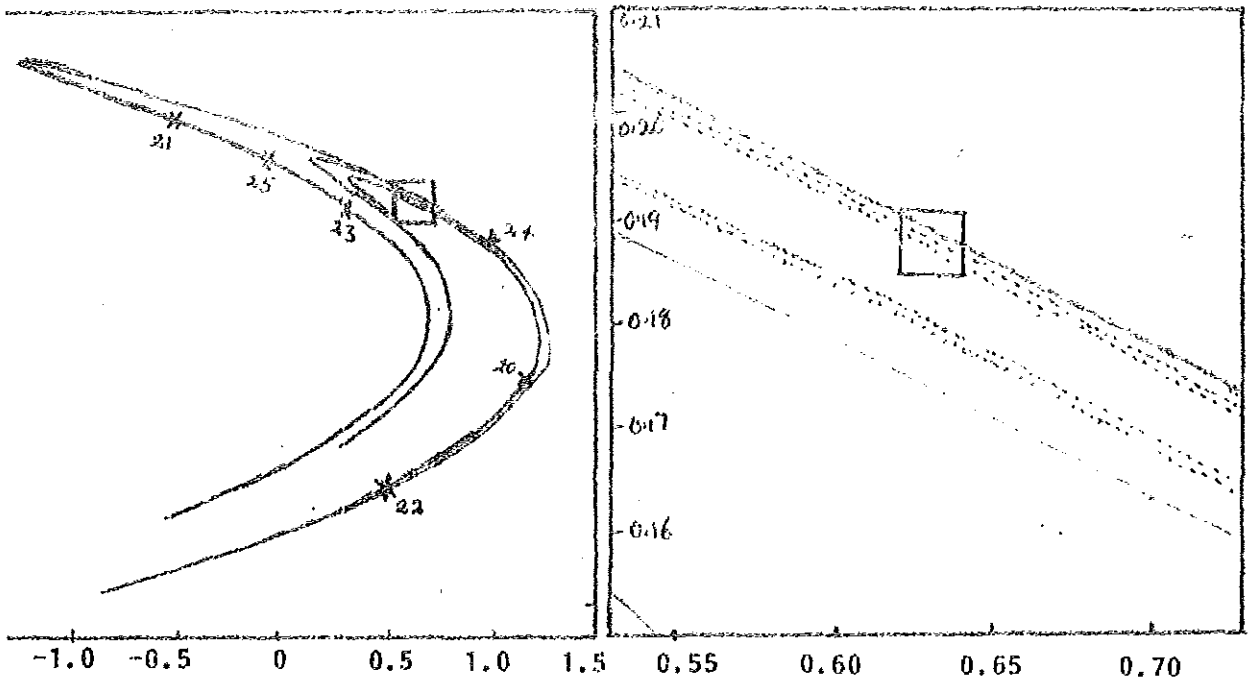

Fig. 4.4: Henon attractor.

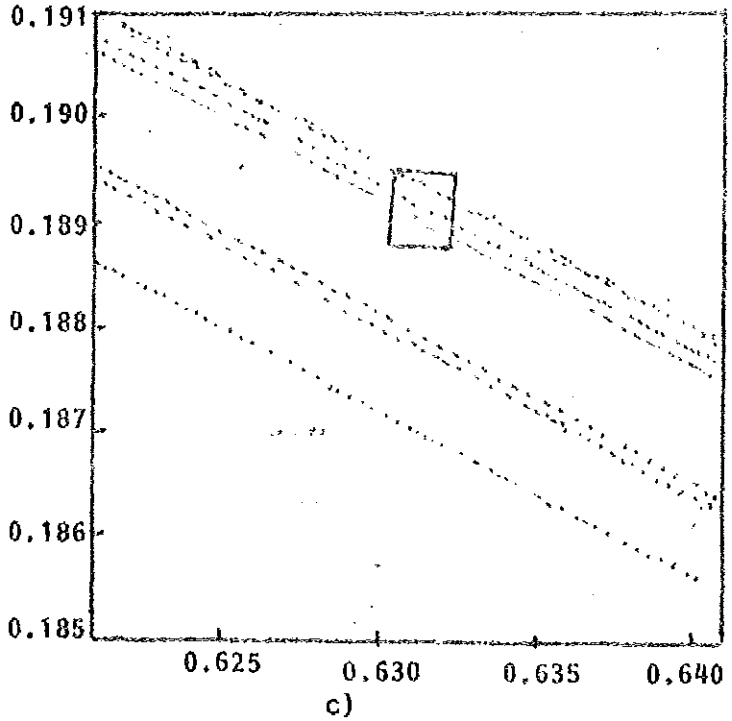

Enlargement of the sequence in (b) 10^6 iterations

4.2 Strange Attractors and the Onset of Turbulence

We come now to one of the most fascinating and difficult questions: how the onset of fluid turbulence in time is related to the emergence of a strange attractor.

We have seen that a dynamical system can be written in the form

$$\frac{d}{dt}X(t) = G_r(X(t)) \qquad (4.10)$$

where r is a parameter which indicate the intensity of the external action on the given system. For example, r ≒ Reynolds number. If r = 0, i.e., if there is no external action, the fluid tends to a state of rest $X(t) = X_o$. This state corresponds to an attracting fixed point X_o for our dynamical system. For small r one observes again a steady state $X(t) = X_r$. As r is further increased, one often sees periodic oscillations in the fluid. This means that asymptotically

$$X(t) = f(\omega t) \qquad (4.11)$$

where f is a function of period 2π and ω is the frequency of the oscillation. This situation correspond to a periodic attractor for continuous time, i.e., a circle or "attracting limit cycle". For sufficiently large r, the fluid motion becomes irregular, chaotic: turbulence has set in [1].

To understand the new route taking to turbulence we have first to introduce a Hopf bifurcation (Hopf, 1942).

A simple Hopf bifurcation generates a limit cycle starting from a fixed point [10]

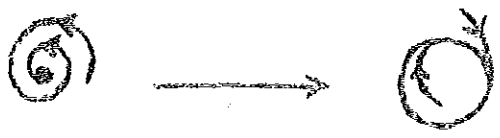

Fig. 4.5: Hopf bifurcation

4.2.1 Landau's Route to Chaos

As early as 1944 Landau suggested a route to turbulence. According to this theory, the time evolution of a turbulent fluid is asymptotically given by

$$X(t) = \lim_{k\to\infty} f_k(\omega_1 t, \omega_2 t, \ldots, \omega_k t) \qquad (4.12)$$

where f_k is a periodic function of period 2π in each of its arguments, and $\omega_1, \omega_2, \ldots, \omega_k$ are independent frequencies [1]. A Hopf bifurcation introduces a new fundamental frequency w into the system. Therefore he suggest that chaotic state is approached by infinite sequence of Hopf instabilities, as shown in Fig. (4.6) [4],[6].

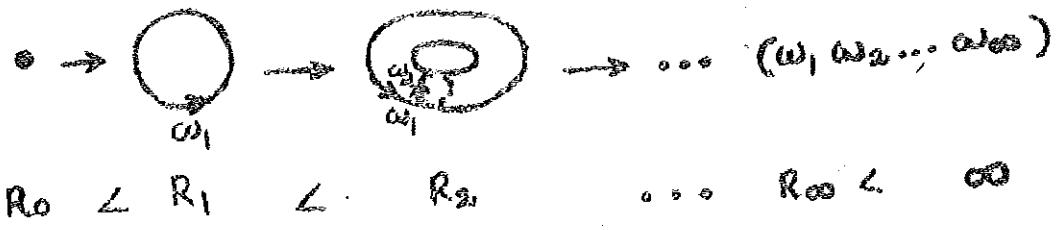

Fig. 4.6: Landau's route to chaos. as the parameter r increases, more and more fundamental frequencies are generated.

A function of t of the form Eq. 4.12 is called quasiperiodic. A quasiperiodic function has a non periodic, irregular aspect, suggestive of turbulence. However, a small change in initial conditions simply replaces $\omega_1 t, \ldots, \omega_k t$ by $\omega_1 t + \alpha_1$, $\omega_2 t + \alpha_2, \ldots, \omega_k t + \alpha_k$ with small $\alpha_1, \alpha_2, \ldots, \alpha_k$. There is thus no sensitive dependence on the initial conditions [1].

Although this route leads to a time dependence which become more and more complicated as more and more frequencies appear, the power spectrum always is discrete and approaches the continuum limit only after an infinite sequence of Hopf bifurcations.

4.2.2 Ruelle-Takens-Newhouse Route to Chaos

The Landau's route to chaos is not in accord with the experiment, for example Bens experiment, after the appearance of two fundamental frequencies, the power specturum becomes contineous. There is no progressive acumulation of many independen discrete frequencies. So it seems that the onset of turbuence may well correspond to the appearance of strange attractors [1].

Ruelle and Takens (197) showed that even after two Hopf bifurcations regular motion becomes highly unstable in favor of chaotic motion at a strange attractor [4]. Newhouse, Ruelle and Takens (1978) showed that a strange attractor is not only possible but generic, that is practically unavoidable, after two Hopf bifurcations, as shown in Fig. 4.7. It is understandable that chaotic motion only becomes possible after two Hopf bifurcations when the trajectory can explore additional dimensions.

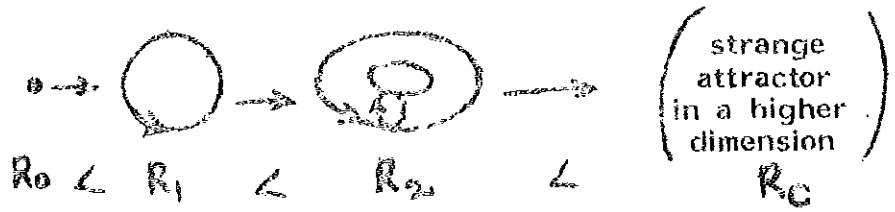

Fig. 4.7: The Ruelle-Takens-Newhouse route to chaos.

Let us discuss one evidence that the sequence to a strange attractor via this route can occur. Curry (1978) considered the same physical problem as Lorenz but he retained greater number of Fourier spatial modes before truncating the series. The result is 14 coupled ordinary differential equations He finds that chaotic time dependence is preceded by doubly periodic motion on a two dimensional toroidal surface which is embedded in the full 14-

dimensional phase space. The torus is found by using the surface of secton technique. A surface of section x_1 = constant was chosen, and another two of the 14 variables, which we denote by x_2 and x_3, were singled out. Every time the orbit crossed the surface of section the x_2, x_3 coordinates of the crossing point were plotted. Fig. 4.8 shows a typical result for the case where a doubly periodic orbit exists; all the points lie on a closed curve. This is the result to be expected for doubly periodic behavior, since the intersection of a torus with a plane (the surface of section) is a closed curve [4].

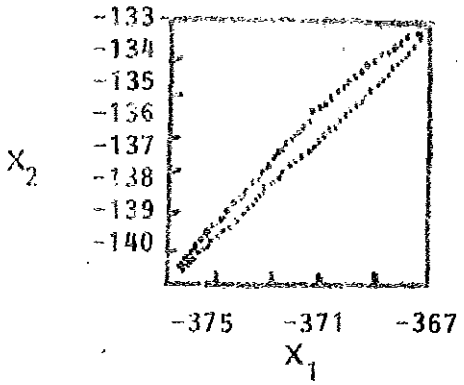

Fig. 4.8: Orbit intersections with the surface of section. (After Curry 1978)

4.3 Experimental Evidence for Ruell-Takens-Newhouse route to chaos

The appearance of the Ruelle-Takens-Newhouse route to chaos after two Hopf bifurcations is demonstrated experimentally in Rayliegh-Benard Convection and Couette flow Fig. 4.9[19].

4.3.1 Benard Experiment

In this experiment the power spectrum for the convection current contineous after the appearance of only two fundamental frequencies, F 4.9a.

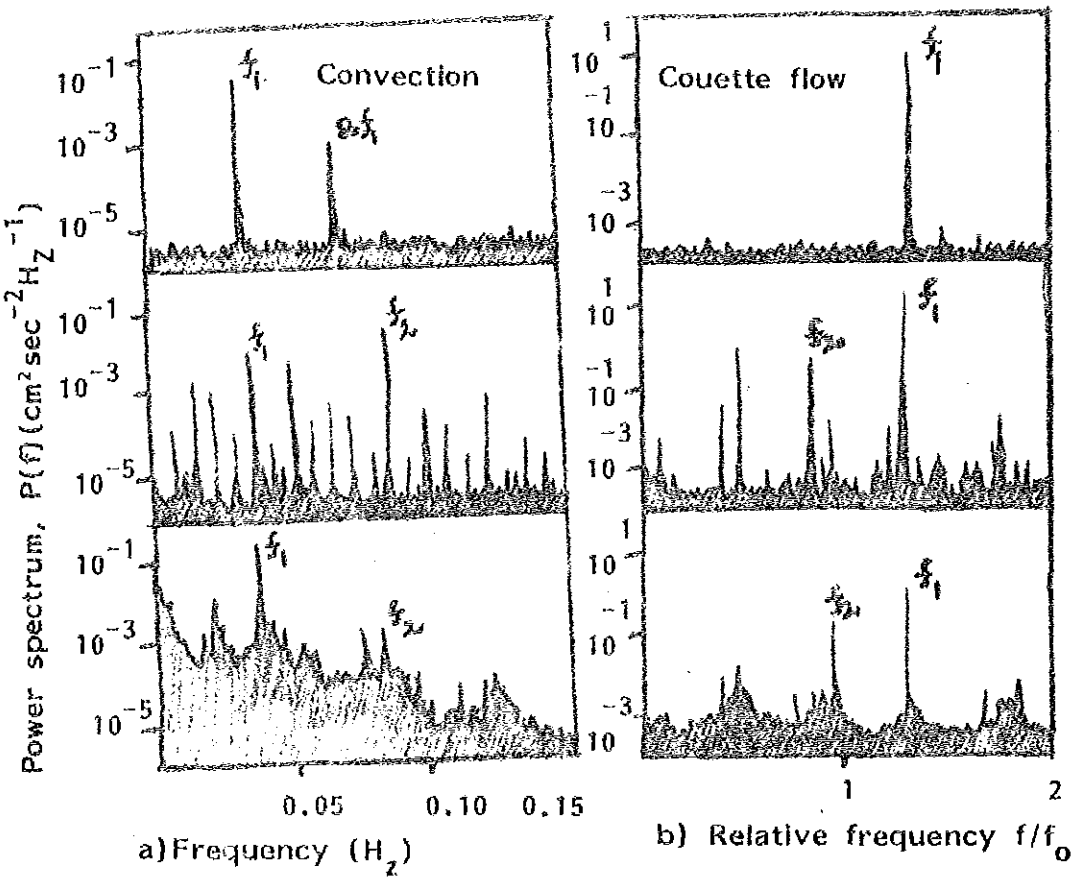

Fig. 4.9: Power Spectrum for Convection and Couette Flow.

4.3.2 Benard Instability

Again in a Benard Experiment, Dubois and Berge (1982) observe the emergence of a strange attractor. They measured the time series of temperature T(t) and reconstructed a two dimensional Poincare section

plotting $(\dot{T}(t), T(t))$ at intervals $t = n\tau$, where τ is determined from an independent measurement of the velocity. Fig. 4.10 shows how the Poincare section, which consists of a closed loop (as expected for a section of a torus), develops into a strange attractor, as predicted by Newhouse, Ruelle, and Takens (1978)[6].

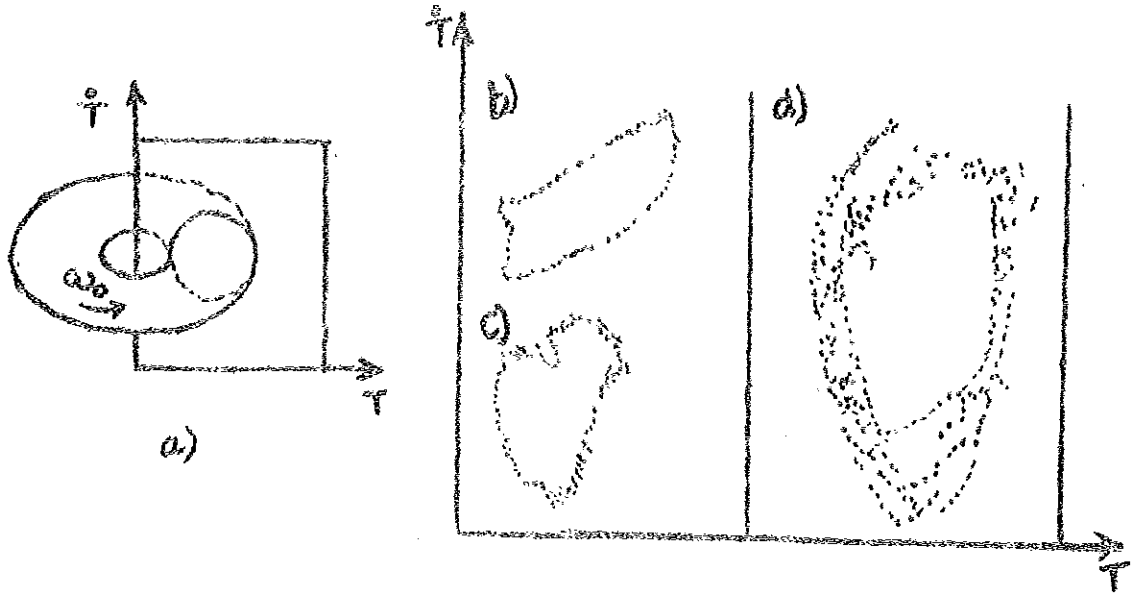

Fig. 4.10: Poincare sections for the Benard Experiment

Fig. 4.10(b) - (d) shows a transition from quasiperiodic motion (b) to substractures indication the destruction of the torus (c) and then to a strange attractor (d), as one increases the Rayliegh number.

4.3.3 Taylor Instability

The Taylor instability occurs in a fluid layer between an inner cylinder rotating with angular velocity ω and a stationary outer cylinder, a geometry known as "circular Couette flow"[19]. For small ω, angular momentum fed

to the inner cylinder is transported outside by viscosity. Above a critical angular velocity ω_c this state becomes unstable and momentum is transported by annular convection cells. At still higher ω's periodic and multiperiodic oscillations of these cells occur which merge into chaos after two Hopf bifurcations, Fig. 4.9b. This confirms again the Ruelle-Takens-Newhouse route to chaos is involved.

By reconstructing the phase space for a Taylor experiment from a time series of the radial velocity $\{ V(t_k),\ldots,V(t_k+m\tau)$ with $t_k = K\tau_o$, $K = 0,1,2,..$ $(\tau_o < \tau)$, We get a Poincare section with a break up of the torus Fig. 4.11, similar to Fig. 4.10[6].

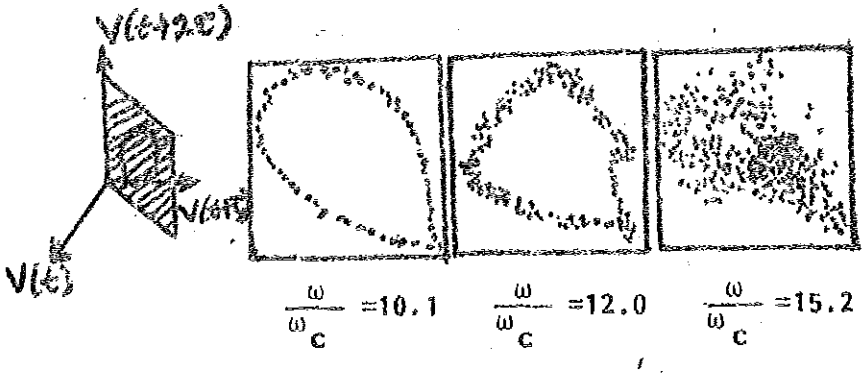

Fig. 4.11: Plane of the Poincare section and break up of the torus with increasing ω.

4.4 Summary of Routes to Chaos

Up to now we have seen three routes to chaos: The Feigenbaum route, Intermittency, and the Ruelle-Takens-Newhouse route. All these three routes and their distinctive features are given in table 3. However, one should not take them as the only routes to chaos. They are simply the

prominent scenarios which have had theoretical and experimental success. One should hope that further relevant scenarios will be found in the future.

Table 3. Summary of the three routes to chaos

Feigenbaum	Manneville-Pomeau	Ruell-Takens-Newhouse
Pitchfork bifurcations	Tangent bifurcations	Hopf bifurcations
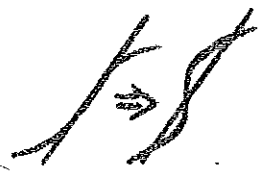	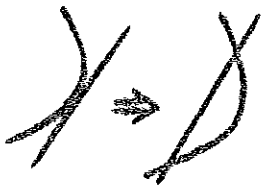	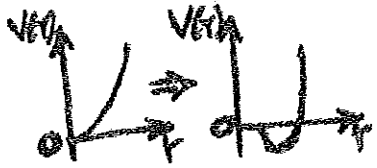
Bifurcation Diagrams		
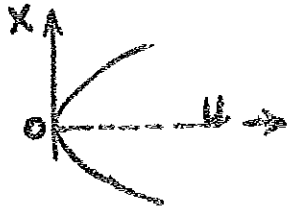	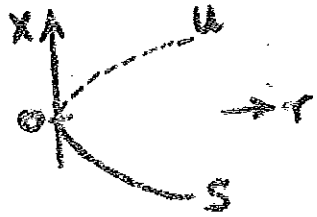	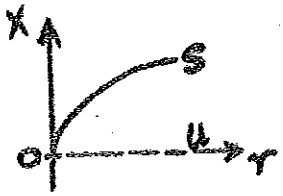
Main Phenomena		
Infinite casecade of period doubings with universal scaling parameters	Intermittent transition to chaos. The laminar phase has duration $(r-r_c)^{-\frac{1}{2}}$	After three bifurcations strange attractor "probable"
Experiments		
Benard Experiment Taylor Experiment Driven nonlin. Oscill. Chemical reactions Optical instabilities	Benard Experiment Josephson junction Chemical reactions Lasers	Benard Experiment Taylor Experiment Nonlinear Conductors

5. Chaos in Conservative Systems

We have dealt upto now with dissipative systems. But there exists in nature a large class of physical systems for which chaotic motion has been found before the discovery of strange attractors in dissipative systems. These are conservative systems which encompass all dynamical systems of classical mechanics.

Conservative systems are considered to be either systems which follow Hamilton's equations of motion, and for which volume elements in phase space are conserved or in a more general case, volume preserving, discrete maps.

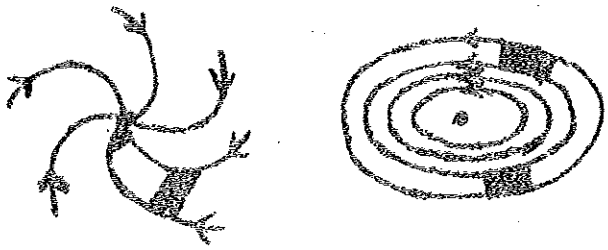

The fact that volumes do not change in conservative systems implies that they display no strange attractors. Nevertheless, in conservative systems one also finds chaotic regions which are not attractive.

5.1 Non-Integrable Versus Integrable Hamiltonian Mechanics

The equations of motion for a system of N-degrees of freedom are obtained from a Hamiltonian, H, as:

$$\dot{q}_k = \frac{\partial H(q,p)}{\partial p_k} \quad , \quad \dot{p}_k = -\frac{\partial H(q,p)}{\partial q_k} \tag{5.1}$$

with $k = 1,\ldots,N$ and $(\vec{\dot{q}})_k = \dot{q}_k$. These are, in general, 2N coupled non-linear first order differential equations. A change of variables from $\vec{q}$, $\vec{p}$ to $\vec{Q},\vec{P}$, is called a cononical transformation if the transformed equation of motion (5.1) for $\vec{Q}$, $\vec{P}$ have the same appearance as (5.1), using the transformed $H'(\vec{Q};\vec{P})$. A particular popular canonical transformation is the one to Action-and-Angle variables, $\vec{J}$ and $\vec{\Theta}$ [20]. These new variables are defined as variables which will transform the given $H(\vec{q},\vec{p})$ into an $H'(\vec{J})$, i.e. one which does not depend on half of the new variables $\vec{\Theta}$. Using this transformation the new equations of motion will be

$$\dot{J}_k = \frac{\partial H'(\vec{J})}{\partial \Theta_k} = 0, \Longrightarrow \vec{J}(t) = \vec{J}(0), \text{ constant} \qquad (5.2)$$

$$\dot{\Theta}_k = \frac{\partial H'(\vec{J})}{\partial J_k} \equiv w_k(\vec{J}) \Longrightarrow \vec{w} \text{ is a constant} \qquad (5.3)$$

Thus, $\Theta_k(t) = w_k t + \Theta_k(0)$,

i.e. we have explicitely, and trivially integrated the equations of motion and obtained 2N constants of the motion $\vec{J}$, $\vec{\Theta}(0)$. Hence, a Hamiltonian system is called integrable if we can obtain these action and angle variables as a function of $\vec{q}$, $\vec{p}$.

One can also use the canonical perturbation theory to distinguish whether the system is integrable or not [21]. The transformation to action angle variables is a subject of this theory. That is, one writes each of the old variables $q_1,\ldots,q_n$, $P_1,\ldots,P_N$ as a power series, Birkhoff series, in all new variables $J_1,\ldots,J_n$, $\Theta_1,\ldots,\Theta_N$. The as yet unknown coefficients in the series are derived by substituting the series into $H(\vec{q},\vec{p})$ and the equation of motion (5.2-3), up to the lowest order terms in $\vec{J},\vec{\Theta}$, we can solve for the lowest order coefficients. Having obtained these we

start all over and obtain the next higher-order coefficients, etc. Hence, whenever the series obtained do converge we have an integrable system by definition, and we have the $\vec{q},\vec{p}$ as explicit functions of the constants $\vec{J}$ and $\vec{\theta}$.

The above iterative procedure, however often breaks off due to one coefficient acquiring a zero denominator. This signals that we either need another variant of Birkhoff series or that no truly convergent series exists at all, i.e. one of the integrals is a singular function of q,p. In the latter case the system is called Non-Integrable. Thus, whenever we have infinite Birkhoff series the system is integrable if the series converges or non-integrable if the series diverges.

One of the simplest example of an integrable system is the harmonic oscillator with a Hamiltonian.

$$H = \tfrac{1}{2}(p^2 + \omega^2 q^2) \tag{5.5}$$

From this we can show that

$$H(J) = J\omega$$

$$J = -\frac{\partial H}{\partial \theta} = 0 \longrightarrow J = \text{const.} \tag{5.6}$$

$$\dot{\theta} = \frac{\partial H}{\partial J} = \omega \longrightarrow \theta = \omega t + \theta(0) \tag{5.7}$$

The motion in the variables p and q is

$$q = \left(\frac{2J}{\omega}\right)^{\frac{1}{2}} \text{Cos}\,\theta \quad , \quad P = -(2J\omega)^{\frac{1}{2}} \text{Sin}\,\theta \tag{5.8}$$

The corresponding trajectory in phase space is an ellipse which become a circle with polar coordinates $J^{\frac{1}{2}}$ and θ after proper rescaling. Comparing Eqns. (5.2-4) and (5.6-7) one can see that the equations of motion (in action-angle variables) of any integrable system with N degrees of freedom are practical

the same as those of a set of N uncoupled harmonic oscillators. The only difference is that in a general integrable system the frequencies ω_i are still funcitons of the actions J_i whereas they are independent of J_i for harmonic oscillators. In analogy with the harmonic oscillator, the existance of n integrals of motion $(J_1,\ldots,J_N)$ confines the trajectory in the 2N-dimensional phase space of an integrable system of an N-dimensional torus. The actions $\vec{J}$ measures the N radii of the torus and $\vec{\theta}$ the N angles of a point on the torus.

5.2 Properties of Integrable Systems

We have seen that all integrable systems with N-degrees of freedom can be nonlinearly transformed into each other and are in this sense equivalent to N harmonic oscillator or even to N pendual. Hence we expect their phase planes to look like nonlinearly deformed versions of the phase plane for the pendulum, [20],(21], Fig. 5.1.

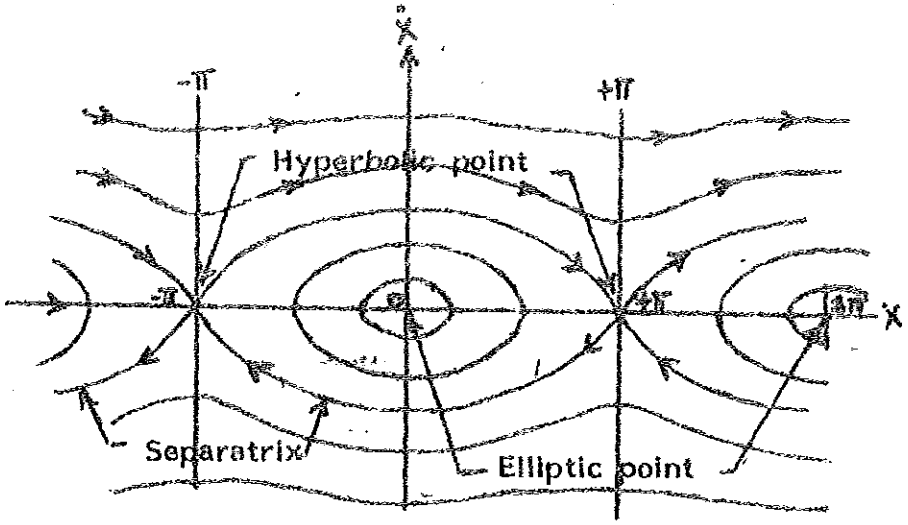

Fig. 5.1. Phase Plot for the Pendulum $\ddot{x} = -\sin x$.

Fig. 5.2 shows the motion of an integrable system with two degrees of freedom, i.e. with 4-dimensional phase space, on a torus, we can generalize this result for higher dimensions.

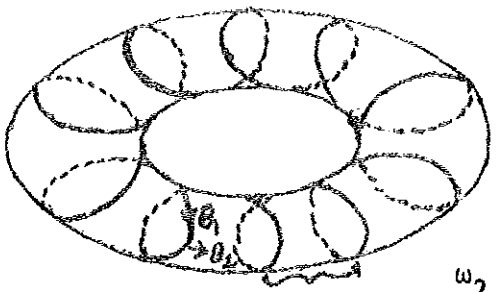

Fig. 5.2 Torus in phase space

colsed orbits occur only if $n\,\Delta\theta_2 = m\,2\pi$, i.e.

$$\frac{\omega_2}{\omega_1} = \frac{m}{n} = \text{rational}; \quad m,n = 1,2,3,\ldots \tag{5.9}$$

for irrational frequency ratios the orbit never repeats itself but approaches every point on the two dimensional manifold infinitesimally close in the course of time [6].

Since each bounded orbit is constrained to a smooth N dimensional torus, it cannot come arbitrarily close to every point on the (2N-1) dimensional surface of constant energy, $N \geq 2$. Hence an integrable system cannot be ergodic ($N \geq 2$), let alone approach thermal equilibrium. In order to be ergodic an orbit should, in general, cover the surface of constant energy both densely and uniformly.

Let us now add to H_o, of an integrable system, a perturbation εH_1.

$$H(\vec{J},\vec{\theta}) = H_o(\vec{J}) + \varepsilon H_1(\vec{J},\vec{\theta}) \tag{5.10}$$

where we expressed H_1 in action-angle variables $\vec{J} = (J_1,J_2)$, $\vec{\theta} = (\theta_1,\theta_2)$ of the unperturbed system.

It is found that the system cannot be integrated by perturbation theory for rational frequency ratios because of strong resonances, and it seems that it can at most be integrated for irrational values of ω_1/ω_2 if the perturbation series in ε converges.

For an integrable system, if $\frac{\omega_1}{\omega_2}$ is close to an irrational number is perturbed by εH_1 then by KAM theorem the system will be stable under the perturbation εH_1 in the limit $\varepsilon \ll 1$. For large ε the perturbation εH_1 destroys all tori [6]. The destruction of this KAM torus shows some similarity to the Ruelle-Takens route to chaos in dissipative systems.

When ω_1/ω_2 is rational, the original torus decomposes into smaller and smaller tori Fig. 5.3. Some of these newely created tori are again stable according to KAM theorem. But between the stable tori the motion is completely irregular [6].

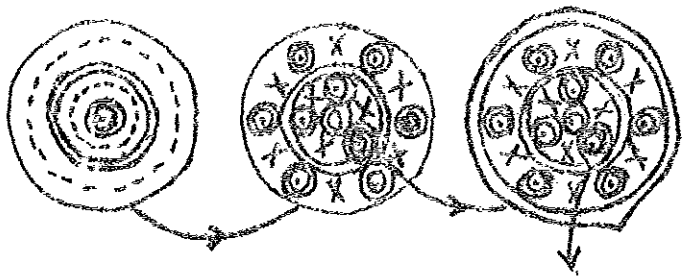

Fig. 5.3: Tori with rational frequency ratio decays into smaller and smaller tori.

5.3 Sensitive Dependence on Initial Conditions and Random Behavior

We saw that for a Nonintegrable system the Canonical Perturbation series, or Birkhoff series, diverge, in all likelihood due to a singularity in one of the integrals $J_k(\vec{q},\vec{p})$. Moreover there appears to be an infinite set of such singularities in phase space [21].

Thus, two orbits with their initial conditions arbtrarily close together, but on different side of such a singularity, can have vastly different behavior. i.e. the orbits depend sensitively on the initial conditions. This dependence is often so sensitive that we cannot calculate the orbit for any time interval of interest, due to experimental or numerical uncertainity in the initial-condition.

As a final point let us mention that Notwithstanding the abundance of chaotic regions, there is also an abundance of regular regions in phase space. This follows from KAM theorem which shows that many of the simple quasi-periodic solutions of an integrable system will still be present, virtually unchanged, in a nonintegrable system, in general. Moreover, a finite fraction (measure) of all orbits are of this regular type [21].

Summarizing, if we disturb the regular orbits of an integrable system on a torus in phase space by adding a non integrable perturbation, then depending on the different initial conditions (different $\vec{J}$, $\vec{\theta}(0)$ in Eqns. (5.2-4) imply different ω_1/ω_2 since $\vec{\omega} = \vec{\omega}(J)$) regular or completely irregular motion results. Although the measure of initial conditions which lead to regular motion is nonzero due to the KAM theorem, for every rational frequency ratio one obtains smaller and smaller stable tori and irregular orbits due to the hyperbolic fixed points. Thus, an arbitrarily small change in the initial conditions leads to a completely different long-time behavior.

5.4 Examples of Classical Chaos

We present some experimental evidence for the coexistence of regular and irregular motion.

1. The Henon-Heiles System

$$H = \tfrac{1}{2}(p_1^2 + q_1^2 + p_2^2 + q_2^2) + (q_1^2 q_2 - \frac{q_2^3}{3})$$

which consists of an integrable pair of harmonic oscillators coupled by non-integrable cubic terms (Henon, Heiles, 1964) [22].

This system has not been solved using any analytic method. Numerical solutions can however be obtained over a time interval of physical interest when sufficiently many numerical precautions are taken. How do we look for possible chaotic behavior in the 4-dimensional phase space of q_1, p_1, q_2, p_2? If we restrict the initial conditions to one value of the energy, E, there are only 3 independent coordinates left over, due to the constraint $H(q_1, p_1, q_2, p_2) = E$. Since 3-dimensional phase space is still difficult to draw we only plot the intersection points of the orbit $q_1(t)$, $q_2(t)$, $p_2(t)$ with a 2-dimensional plane q_2 versus p_2 (at $q_1=0$). If the system were integrable this (Poincare-) surface of section would look like a dotted version of Fig. 5.1, for the Pendulum, i.e dotted elipses, dotted separatrices, etc. Fig. 5.4 shows surfaces of section for the Henon-Heiles system. Inspecting its left column we see that at some low energy, $E = 1/12$, the phase plot does like a dotted deformed version of the one for an integrable system. Note the three most visible hyperbolic points and the separatrices "connecting" them. However, at $E = 1/8$ these seem to have disappeared, replaced by a chaotic collection of dots (from one orbit) through which it would be difficult to draw a nice simple curve. At higher energy $E = \frac{1}{6}$, nearly

all of the available phase plane seems chaotically filled with the intersection dots of just one orbit. Yet some minuscule islands', with an elliptic, i.e., linearly stable point at their center, can still be seen. Those orbits do not wander. A hyperbolic orbit is one that is unstable under linear perturbation.

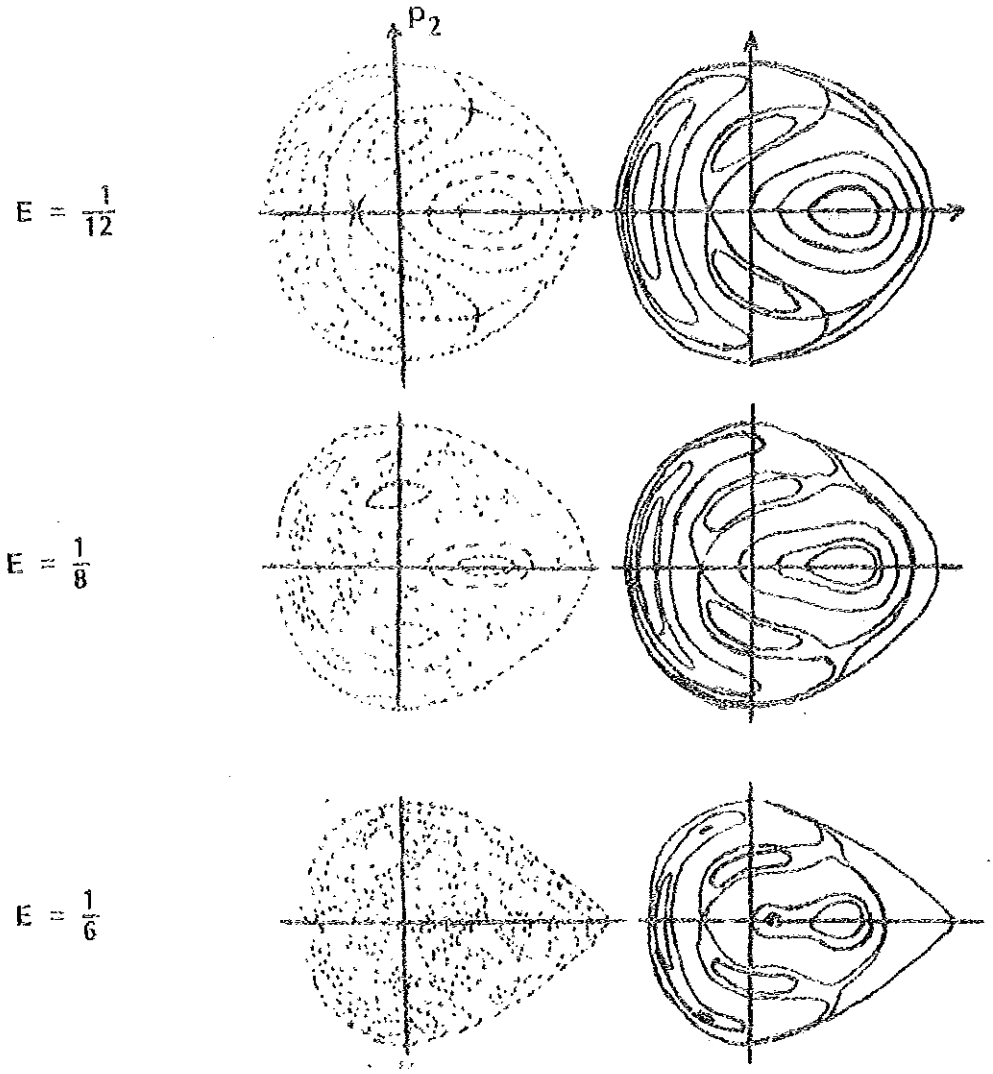

Fig. 5.4: Poincare maps for the Hanon-Heiles System

The right-hand column shows the surfaces of section generated by eighth-order perturbation theory for various energies (after Gustavson, 1966)[21]. The curves agree quite well with the visible behavior of the orbits on the left, at E = 1/12, and several orbits at E = 1/8. However, the choatic "space filling "orbits, visible at E = 1/6 and 1/8, demonstrate that the curves on the right, corresponding to the same initial condition, are incorrect and even misleading as to the qualitative behavior of the orbits. This provides a strong indication that the Henon-Heiles system is non integrable.

2. Motion of an asteroid around the sun, perturbed by the motion of Jupiter.

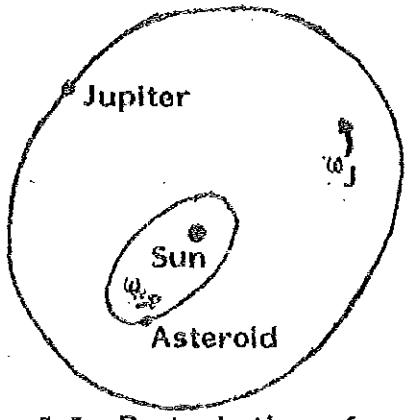

Fig. 5.5: Perturbation of an asteroids motion by Jupiter.

This three body problem is nonintegrable, and from our discussion we expect that the asteriod motion becomes unstable if the ratio of the unperturbed frequency of the asteroid motion ω and the angular frequency of Jupitor ω_j becomes rational. Fig. 5.6 illustrates that, infact, gaps occur in the asteroid distribution for rational ω/ω_J. On the other hand, the existance of stable asteroid orbits ($f \neq 0$) can be considered as a confirmation of the KAM theorem [6].

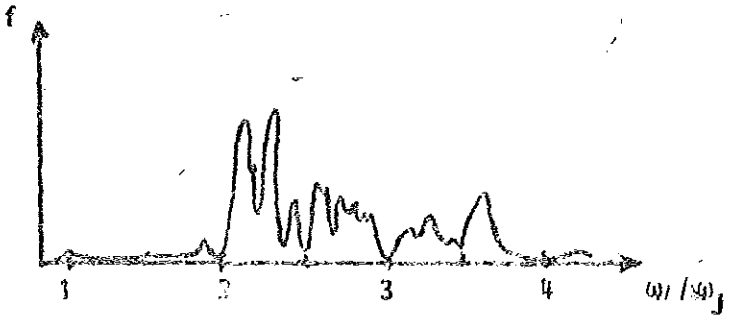

Fig. 5.6 Fraction f of asteroids in the belt between Mars and Jupiter as a function of ω/ω_J (after Berry, 1978)

6. Chaos in Nature Outside Physics

We have seen in chapter 2 the first order difference equation $x_{n+1} = 4bx_n(1-x_n)$ displays regular and chaotic behavior. Then, we have extended this behavior to be observed in any nonlinear system if the given function $x_{n+1} = f(x_n)$, which describes the system, has a single maximum in a unit interval. Based on this (and with some restrictions), we have so many systems outside physics which exhibit similar behavior. Such behavior is found, for example, in ecology: to study a seasonally breeding populations in which generations donot overalp. The theoretician seeks to understand how the magnitude of the population in generation n+1, x_{n+1}, is related to the magnitude of the population in the preceding generation n, x_n. Similar behaviour can be found in genetics where the equaiton describes the change in gene frequency or in epidemiology, where x is the fraction of the population infected at time t = n.

Examples in economics include models for the relationship between commodity quantity and price, for the theory of business cycles, and for the temporal sequences generated by various other economic quantities. Savings account with a self-limiting rate of interest follow the above quadratic equation. The above equaiton, $x_{n+1} = F(x_n)$, is also germane to the social sciences, where it arises, for example, in theories of learning (where x may be the number of bits of information that can be remembered after an interval t = n), or in the propagation of rumours in variously structured societies (where x is the number of people to have heared the rumour after time t = n) [8].

Experiments with animal hearts found another application [9]. It was found the same characteristic pattern which we know from the Feigenbaum diagram.

Climatic variability and the electrical activity of the brain [24] shows also another chaotic phanomena.

7. Conclusion and Implications

In this review work of Nonlinear properties of deterministic systems we have observed the following:

1. We have seen experiments and simple models whose time dependence is deterministic and yet shows chaotic behavior as one varies the external control parameter.
2. We have seen the three prominent routes to chaos which have experimental support.
3. We have observed strange attractors in dissipative systems, Lorenz and Henon attractor, which lead to the exponential separation of initial points on the attractor and lead to chaotic behavior.
4. In conservative systems of classical mechanics it is observed that chaotic and regular motions coexist together in non integrable systems, though the former aboundance is by far larger than regular motion.
5. The above routes to chaos and other chaotic phenomena are not restricted particularly in physics, but they can be found in many nonlinear stystems in other disciplines.

In spite of practical problems to be solved, the ideas presented in this work have obvious applications in many areas. What are the consequences for our knowledge about the reality, because every system in real life is a nonlinear system?

i) One consequence is that the way of thinking should be changed. We should be aware of the fact that chaotic systems in our world are the normal case, not the exception.

It is observed that in the chaotic regime arbitrarily close initial conditio can lead to trajectories which, after a sufficiently long time, diverge widely. This means that, even if we have a simple model in which all the parameters are determined exactly, long term prediction is nevertheless impossible.

This insight should open a new view not only on such simple models, but also on other achievements of human civilization which we have thought to be under our complete controll. After the first excitement caused by the feeling of a partial success we have to learn that the principle of chaotic behavior limits many of our attempts to create an ideal world out of our brain.

ii) Pedagogical. Students should be introduced early to some nonlinear systen such as equation 2.1, in their mathematical education to enrich their intuition.

iii) It appears that an adequate understanding of nature requires much more than finding the fundamental laws. Phenomenological analysis must gain more attention.

REFERENCES

[1] Ruelle, D., Strange Attractors, Math. Intelligencer 2,126 (1980).

[2] Lorenz, E.N., Deterministic Nonperiodic Flow, J. Atoms. Scie. 20, 130(1963).

[3] Hudson, J.L., and Mankin, J.C., Chaos in the Belousov-Zhabotinskii Reaction, J. Chem. Phys. 74, 6171(1981).

[4] Ott, E., Strange Attractors and Chaotic Motions of Dynamical System, Rev. Mod. Phys. 53, 655(1981).

[5] Ford, J., How Random is Coin Toss?, Phys. Today April (1983).

[6] Schuster, H.G., "Deterministic Chaos", Weinheim, Physik-verlag (1984).

[7] Feignbaum, M., Universal Behavior in Nonlinear Systems, Los Alamos Science (1980).

[8] May,R.M., Simple Mathematical Models with Very Complicated Dynamics, Nature 261, 459(1976).

[9] Becker, K.H., Journey into the Land of Infinite Structures, Proceedings of the Int. Workshop on Teaching Nonlinear Phenomena Vol. II, Hungary (1987).

[10] Eckmann, J.P., Roads to Turbulence in Dissipative Dynamical Systems, Rev. Mod. Phys. 53, 643(1981).

[11] Cvitanovich, P., "Universality in Chaos", A reprint selection, Adam Hilger, Bristol (1984).

[12] Libchaber, A., and Maurer, J., A Rayleigh Benard Experiment, Nonlinear Phenomena at Phase Transitions and Instabilities 259(1982).

[3] Arecchi, F.T., Meucci, R., Puccioni, G., and Tredicce, J., Experimental Evidence of Subharmonic Bifurcations, Multistability and Turbulence in a Q-switched Gas Laser, Phys. Rev. Lett. 49, 1217(1982).

[14] Pomeau, Y., and Manneville, P., Intermittent Transition to Turbulence in Dissipative Dynamical Systems, Comm. Math. Phys. 74, 189(1980).

[15] Berge, P., Dubois, M., Manneville, P., and Pomeau, Y., Intermittency in Rayleigh-Benard Convection, J. Phys. (Paris) Lett. 41, L-344(1980).

[16] Pomeau, Y., Roux, J.C., Rossi, A., Bachelart, S. And Vidal, C., Intermittent Behavior in the Belousov-Zhabotinsky Reaction, J. Phys. (Paris) Lett. 42, L-271(1981).

[17] Mandelbrot, B.B., Fractals, Proceedings of the Int. Workshop on Teaching Nonlinear Phenomena, Vol. II, Hungary (1987).

[18] Henon, M., A Two-dimensional Mapping with a Strange Attractor, Comm. Math. Phys. 50, 69(1976).

[19] Swinney, H.L., and Gollub, J.P., The Transition to Turbulence, Phys. Today 31(8), 41(1978).

[20] Goldstein, H., "Classical Mechanics", Addison-Wesley Pub. Comp., Cambridge 42, Mass, USA(1953).

[21] Helleman, R.H.G., Self-Generated Chaotic Behavior in Nonlinear Mechanics, In E.G.D Cohen (eds.): Fundamental Problems in Statistical Mechanics, Vol. 5. North-Hall. Publ., Amsterdam.

[22] Lebowitz, J.L., and Penrose, O., Modern Ergodic Theory, Phys. Today 26(2), 23(1973).

[23] Pflug, A., 300 years After the Principia, Proceedings of the Int. Workshop on Teaching Nonlinear Phenomena, Vol. II, Hungary (1987).

[24] Nicolis, G., and Gaspard, P., Self-Organization, Chaotic Dynamics and the modelling of Complex Systems, Proceedings of the Int. Workshop on Teaching Nonlinear Phenomena, Vol. II, Hungary (1987).